Interlaboratory comparison study on AuNPs

-final report-

WG2 - Analytical Toolbox

COST Action ES1205 ENTER

Abstract

An interlaboratory comparison study on the analysis of gold nanoparticles (AuNPs) among members of the working group 4 (engineered nanomaterials) (http://www.norman-network.net/?q=node/54) within the NORMAN network and members of the COST Action ES1205 ENTER (www.es1205.eu) was conducted. The nanomaterials under investigation were gold nanoparticle suspensions (Au NP) with Au NP sizes of 10, 50 and 250 nm. Three monomodal samples and two mixtures (bi- and trimodal) out of the single sized Au NP standards were prepared as (artificial) samples and sent to the attendees for analysis. The aim of the interlaboratory test was to investigate, if comparable data in terms of "easy to handle nanomaterials" and different analytical techniques can be obtained and, if the current EU definition recommendation for the term "nanomaterial" is implementable. Each attendee was free to decide which sample preparation protocol and technique to apply - no strict rules were defined.

Upon a previous survey by means of a questionnaire the available lab equipment of the attendees was assessed. Also based on accessible lab equipment it was asked for following parameters to be analyzed:
i) total concentration of gold in each sample, ii) size distribution of Au NPs in the monomodal samples and in the mixtures, iii) based on the data obtained, decision whether the mixture can be allocated to nanomaterial or not according to the EU definition recommendation [1].

This report compiles the obtained results and findings are discussed in a comparative manner. Pros and cons of the applied techniques are highlighted.

Introduction

Within the frame of the COST Action ES1205 "ENTER" ("Engineered Nanomaterials from wastewater Treatment and stormwatEr to Rivers") and the working group 4 (Engineered Nanomaterials) of the Norman Network an interlaboratory comparison study (ICS) on characterizing engineered gold nanoparticles (Au NPs) was organized and conducted. In total, 12 laboratories participated in the ICS. The study was performed from December 2014 to January 2015.

Five different samples of commercially available Au NP standards (citrate stabilized; suspended in deionized water) (EM.GC 10/50/250, BBIsolutions, Cardiff, UK) and one blank (deionized water) were sent simultaneously to all participating laboratories. The samples contained either Au NPs of one size (samples 1 – 3) or mixtures of different sized Au NPs (samples 4 and 5) (Table 1).

Table 1: Overview of the artificial Au NP samples

	Nominal Size* **[nm]**	**Volume fraction** **[%]**	**Number based concentration*** **[particles/mL]**	**Particle based fraction** **[%]**	**Mass based concentration*** **[mg Au/L]**
Sample 1	250	100	3.6×10^{8}	100	56.8
Sample 2	50	100	4.50×10^{10}	100	56.8
Sample 3	10	100	5.70×10^{12}	100	57.6
Sample 4	10	30	1.71×10^{12}	98.7	17.3
	50	50	2.25×10^{10}	1.3	28.4
	250	20	7.20×10^{7}	0.004	11.4
	Total		*1.73×10^{12}*		*57.1*
Sample 5	50	5	2.25×10^{9}	86.8	2.84
	250	95	3.42×10^{8}	13.2	54.0
	Total		*2.59×10^{9}*		*56.8*

*** based on information obtained from Au NP standard supplier**

The samples should be analyzed for

- particle size
- total Au content
- number-based and/or mass-based particle size distribution.

Furthermore, it should be decided

- whether the bi- and trimodal samples (sample 4, 5) were nanomaterials or not on basis of the definition of the term "nanomaterial" by the European Union: *"A natural, incidental or manufactured material containing particles, in an unbound state or as an aggregate or as an agglomerate and where, for 50 % or more of the particles in the number size distribution, one or more external dimensions is in the size range 1 nm - 100 nm. In specific cases and where warranted by concerns for the environment, health, safety or competitiveness the number size distribution threshold of 50 % may be replaced by a threshold between 1 and 50 %. By derogation from the above, fullerenes, graphene flakes and single wall carbon nanotubes with one or more external dimensions below 100 nm should be considered as nanomaterials"* [1].

No common operating procedure and/or analysis technique was suggested for characterizing the Au NP samples. Each participant conducted the analysis based on own protocols and available techniques. An overview of the applied analytical techniques is given in Table 2.

Table 2: Overview of applied analytical techniques

Method	Abbreviation	Nr. of participants applying the method in the ICS
Nanoparticle tracking analysis	NTA	4
Inductively coupled plasma-mass spectrometry in single-particle mode	sp-ICP-MS	5
Dynamic light scattering	DLS	6
Atomic force microscopy / transmission electron microscopy	AFM/TEM	3
Inductively coupled plasma-mass spectrometry/optical emission spectrometry	ICP-MS/OES	6
Asymmetric flow-field flow fractionation	AF4	2
Chronoamperometry (Electrochemical method)		1
Hydrodynamic chromatography	HDC	1
Laser-induced breakdown-detection	LIBD	1

Based on the outcomes of the interlaboratory comparison study, following specific topics and questions should be addressed and discussed:

- Are the results from identical analytical methods comparable?
- What are/might be the reasons leading to different results (with respect to comparing results from both, same analytical techniques and different analytical techniques).
- Which method parameters are critical for reliable analysis?
- What are the benefits and limitations of each method?

In addition, with the background of the analytical challenges encountered when analyzing NPs in aqueous matrices, the applicability of the suggested EU definition of the term "nanomaterial" should be assessed:

- Is a certain method suitable for a decision "nanomaterial: yes or no?" based on the EU definition?
- Is a technique or a minimal set of techniques available which is sufficient for deciding whether a sample is a nanomaterial or not?

The outcomes and results have been compiled and discussed by the participants of the interlaboratory comparison studies and are presented in this report.

Attendees

In total 12 attendees/institutions joined the ICS. Figure 1 displays the respective number of institutions related to the respective European country:

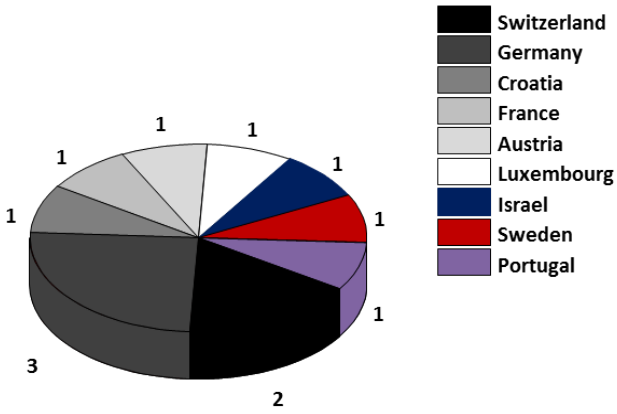

Figure 1: Distribution of attendees/institutions from several countries in Europe.

Table 3 lists the respective institutions and representatives as well as linked numbers uniformly applied within the report.

Table 3: Attending Institutions and Representatives. # are continuously and uniformly linked with the respective Institution and representative within the whole report

Attendee #	Institution	Representative
1	CRP Gabriel Lippmann – Luxembourg	Tommaso Serchi & Sebastien Cambier (Serchi@lippmann.lu)
2	Gothenburg University – Sweden	Geert Cornelis (geert.cornelis@slu.se)
3	Institute Ruđer Bošković – Croatia	Irena Ciglenečki & Marija Marguš (irena@irb.hr)
4	Institute for environmental sciences, University of Koblenz/Landau – Germany	Allan Philippe (philippe@uni-landau.de)
5	Institut Agroscope – Switzerland	Thomas Bucheli & Alexander Gogos (Alexander.Gogos@eawag.ch)
6	University of Vienna – Austria	Frank v.d. Kammer & Stephan Wagner (frank.von.der.kammer@univie.ac.at)
7	DVGW-Technologiezentrum Wasser (TZW) – Germany	Martin Tröster (martin.troester@tzw.de)
8	Eawag – Switzerland	Ralf Kaegi (Ralf.Kaegi@eawag.ch)
9	Institut de Physique du Globe de Paris – France	Mickaël Tharaud & Yann Sivry (sivry@ipgp.fr)
10	Weizmann Institute of Science – Israel	Ilit Cohen-Ofri (ilit.cohen-ofri@weizmann.ac.il)
11	Instituto Superior Técnico – Portugal	Rute Isabel Ferreira Domingos (rdomingos@ipgp.fr)
12	Federal Institute of Hydrology - Germany	Björn Meermann (meermann@bafg.de)

In the following paragraphs the results are shown and discussed.

References:

[1] EU, Commission recommendation of 18 October 2011 on the definition of nanomaterial (2011/696/EU). Official Journal, 2011a, **L 275**, 38-40.

I NTA

I.1 Theoretical background of NTA

The NTA technique relies on the light scattered from particles undergoing Brownian motion. Individual particle trajectories are tracked in real time using an optical microscope and the mean squared distances that are traveled by the particles in two dimensions are determined and analysed by the NanoSight software in order to determine number-based diffusion coefficients. The mean size corresponds to the arithmetic average of all particle sizes while the modal size corresponds to the most frequently observed particle diameter. Since the scattering of small particles varies strongly with particle radius, larger particles can mask the signal of the smaller nanoparticles, however, this effect is less important than in DLS.

I.2 Participants and analytical measures

In total four of the laboratories which participated at the ICS analysed the samples by NTA (#1, #4, #11, #12). Following instruments and cameras were used by the participants:

- #1: NTA NS500; Scientific CMOS Trigger
- #4: NTA LM20; CCD camera (8 bit, 640×480, 30 frames per seconds)
- #11: NTA LM10; Scientific CMOS Image Sensor
- #12: NTA LM10; Camera: MARLIN F033B (1/2” progressive scan CCD)

I.3 Sample preparation

The samples were treated and prepared for the measurement as follows:

- *#1*

  The Au stocks were kept in the fridge from the moment that they arrived. The NTA analyses were carries out at room temperature, 21 ºC. When needed the stocks were diluted in MilliQ water.
  The solutions were mixed by vortexing. Fresh dilutions were prepared every day for the replicates. Samples were loaded by the NanoSight pump.

- *#4*

  The Au stocks were kept in the fridge from the moment that they arrived. The NTA analyses were conducted at room temperature, 22 ºC. When needed the stocks were diluted in MilliQ water.
  No mechanic agitation/stirring of the solution was used; only shaken by hand. Samples were injected with a polypropylene syringe.

- *#11*

  The Au stocks were kept in the fridge from the moment that they arrived. The NTA analyses were done at room temperature, 21 ºC. When needed the stocks were diluted in MilliQ water.
  No mechanic agitation/stirring of the solution was used; only shaken by hand. Fresh dilutions were prepared every day for the replicates. Samples were injected with a polypropylene syringe.

- *#12*

  The Au stocks were kept in the fridge from the moment that they arrived. The NTA analyses were carried out at room temperature, 21-22 ºC. When needed the stocks were diluted in MilliQ water. Samples were shaken overhead at 40 rpm during 15 min. Samples were injected with a polypropylene syringe.

The dilution factors used for the measurements are stated in Table I.1.

I.4 Results and discussion

The results obtained by the participants are shown in Table I-1.

Monomodal samples

Size: in general for the samples with larger sizes, 50 and 250 nm, the mean and mode diameters are in accordance, which is also independent of the stock dilutions performed by the attendees (ranged from 0 to 251×), and in reasonable accordance with the nominal sizes of the particles. In fact, a point of discussion can be raised with the fact that some attendees needed to dilute their samples and others not. Most probably, related with the different aggregation states of the received particles, and more important due to the set gain & shutter chosen; there are 16 camera levels ranging from less sensitive (level 1: gain = 0 & shutter = 1), to the most sensitive (level 16: gain = 512 & shutter = 1300). Attendee 1: sample -: gain = 1 & shutter = -; sample 2: gain = - & shutter = -. Attendee 4: sample 1: gain = 1 & shutter = -; sample 2: gain = 1 & shutter = -. Attendee 11: sample 1: gain = 200 & shutter = 800; sample 2: gain = 300 & shutter = 500. Attendee 12: sample 1: gain = 20 & shutter = 400; sample 2: gain = 50 & shutter = 1300.

For the 10 nm sample three of the attendees found agglomerates with more than 100 nm, whereas one of the attendee obtained sizes lower than 100 nm but much larger than the nominal size of the particles (mean: 83 nm, mode: 48 nm *vs.* 10 nm for nominal size). The absence of signal for the single 10 nm particles is related to the limit of detection of the instrument.

Concentration of particles: overall all attendees obtained different values for the different particle suspensions (including the mixtures), which is most probably a consequence of the impossibility to calibrate the volume and unexpected aggregation/attachment of nanoparticles for samples received by some attendees.

Table I-1: Number-based particle concentrations and diameters (mean; mode) obtained using NTA from 4 attendees, including the dilution factor for each sample by using MilliQ water as dilution media

	#1			#4			#11			#12		
Sample	**Dil**	***C* /part mL^{-1}**	***d* /nm**	**Dil**	***C* /part mL^{-1}**	***d* /nm**	**Dil**	***C* /part mL^{-1}**	***d* /nm**	**Dil**	***C* /part mL^{-1}**	***d* /nm**
$Au_{250\ nm}$	0	4.50×10^{8}	240; 243	0	2.81×10^{8}	251; 242	34.3×	5.45×10^{9}	196; 144	0	1.26×10^{9}	280; 267
$Au_{50\ nm}$	2500×	1.98×10^{11}	61; 47	101×	6.16×10^{10}	64; 54	251×	1.03×10^{11}	99; 49	21×	1.21×10^{9}	91; 51
$Au_{10\ nm}$	0	1.54×10^{8}	83; 48	0	3.22×10^{8}	156; 114	84.3×	1.89×10^{10}	187; 104	0	1.20×10^{8}	108; 63
$Au_{10,50,250\ nm}$	1000×	1.56×10^{11}	57; 47	101×	6.83×10^{10}	55; 50	251×	6.77×10^{10}	99; 50	21×	7.14×10^{8}	92; 53
$Au_{50,250\ nm}$	100×	1.93×10^{10}	77; 48	11×	3.77×10^{9}	263; 240	51×	1.31×10^{10}	181; 68	11×	2.30×10^{8}	254; 261

Bi- and trimodal samples

Size: for the mixture containing the 10 nm particles (sample 4) the attendees obtained in general the same size, around 50 nm, which corresponded to the size of the main Au NP fraction in mass corresponding to 2.25×10^{10} particles per mL, whereas 1.71×10^{12} and 7.20×10^{7} particles per mL should be present for the 10 and the 250 nm particles, respectively. Most probably the 50 nm particles hide the smaller NPs (or they really cannot be detected due to the NTA detection limit), whereas too few 250 nm particles were present after dilution to be detected in significant amount.

For sample 5 containing 5% in volume of 50 nm particles and 95% of 250 nm particles three of the attendees obtained sizes in the same order of magnitude in accordance with the largest size present in the mixture, whereas one attendee obtained values below 100 nm much closer to the 50 nm particles.

In fact data for monomodal samples from different attendees were comparable. The comparison of data obtained with the LM10 or 20 (4, 11 and 12) shows that in general the handling of the sample, including the dilution factor is not of critical importance for size determination as far as enough particles are detected.

The given concentrations are not credible due to the absence of volume calibration and high standard deviations. If a symmetrical distribution is expected, an indicator of aggregation can be obtained by comparing mean and mode values: larger mean values compared with mode values suggest partial aggregation of the sample. However, the settling of the NPs between the injection and the recording can overestimate this difference. From the data obtained it seems crucial not only to look to the mean and mode values but also critically to observe the distribution curve in order to evaluate the presence or not of small populations of particles with different sizes.

The ranking of the NTA technique is in fact unclear in that it should provide number average diameters (similar to the microscopic techniques) but it can have a bias to track the strongly scattering (i.e., larger) particles (similar to DLS, despite the fact that DLS is much more sensitive towards large impurities than NTA). However, it is of importance to mention that it has the advantage of the possibility to see the particles moving in the volume, which allows to i) choose an optimum particle concentration, ii) observe the heterogeneity on size of the sample despite the fact that when recording the signals the smaller particles were not detectable; thus, it needs to be kept in mind that analysis time needs to be prolonged/adapted then; and iii) critically assess the quality of the raw data (checking the full process of data acquisition and analysis, systematic errors or artifacts). Another advantage is related with the particles concentration to be used, which in general is lower than the one that need to be used in DLS. Moreover, compared with DLS, the NTA can give a more precise number-based size distribution due to the lower amount of hypotheses and computation during the data analysis, and also it has a lower detection limit in terms of particle concentration. However, an important disadvantage of NTA is the “high detection limit” in terms of particle size.

When analyzing NPs by means of NTA, as it also became obvious by the ICS, it is crucial to ensure that the working concentration of the particles is suitable for analysis, i.e. on the one hand that there are enough particles in the detector volume and on the other hand the sample is not too concentrated. Furthermore, the effect of sedimentation should be checked by visualizing the same volume before and after shaking or “turning over” of the sample chamber.

Regarding data assessment it is possible to take the raw data of the diffusion times for each particle detected and use specific equations for different shapes of the particles. For spherical particles the diffusion coefficients and diameters directly obtained by the software seem to be very reasonable. In fact, the last version of the software

allows changing the threshold to be applied in the analysis with the objective to analyze different populations of particles in a heterogeneous size sample (not done here).

I.5 EU definition

In general NTA is not suitable for a decision “Nano: Yes//No” based on the EU definition due to the bias through larger particles (although this seems less important than for DLS) and the high uncertainties related to number-based concentration determination.

II sp-ICP-MS

II.1 Theoretical background of sp-ICP-MS

Single particle inductively coupled plasma-mass spectrometry (sp-ICP-MS) is currently the only technique that addresses the high demands from regulators, industry and scientific community to analyse low number concentrations of metal containing NPs in complex matrices. The principle of sp-ICP-MS is illustrated in Figure II-1. The signal intensity caused by arrival of ion clouds at the detector produced from NPs can be calculated to the mass of the particle and therefore its size, if a spherical shape is assumed, whereas the particle number concentration is calculated from the detected particle burst frequency. The fast measurement frequency of sp-ICP-MS allows counting statistically significant particle numbers from relatively dilute suspensions in a short time and the specificity of ICP-MS allows discerning NP with a specific inorganic composition from other, naturally occurring particles. This feature is especially useful when working in complex matrices such as wastewaters, blood or food where a host of other particles occurs. The only other competitive technique, TEM can, in theory, also determine number concentrations specifically, but requires high particle counts and thus long analysis times to arrive at a statistical significant count. Moreover, TEM suffers greatly from drying artefacts during sample preparation. This poses practical constraints on the total number concentration that can be measured with TEM. Other techniques are similarly insensitive for low number concentrations and more importantly, they cannot distinguish specific particles in a background of many different types of particles.

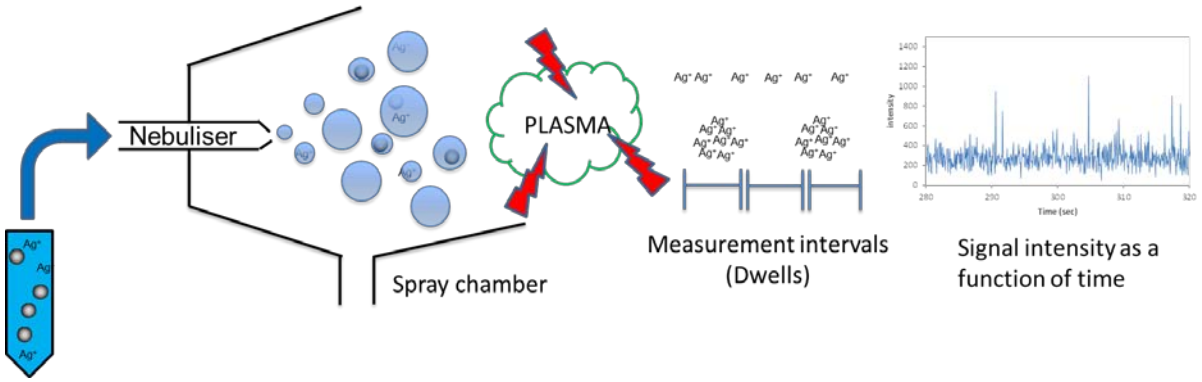

Figure II-1: Principle of sp-ICP-MS. A NP suspension, e.g. silver NPs usually accompanied by dissolved Ag ions are injected via the nebulizer and spray chamber in the plasma where NPs are atomized and ionized into isolated clouds of ions that are detected as sharp peaks at the detector, whereas dissolved Ag produces more or less continuous stream of ions.

II.2 Participants and analytical measures

5 partners joined using different instruments having different sensitivities and also different capabilities in terms of the dwell time used (Table II-1). Other differences are the number of data points used per sample by the different partners. The latter differences arise because software limitations of certain instruments impose additional time of each analysis making it difficult to acquire much data in a short amount of time. At the same time, other software imposes a minimal dwell time of around 3 ms.

The approaches were also different between partners. Most partners made a classical calibration curve of dissolved Au, used a NIST 60 nm or other 60 nm particle (e.g. British Biocell International) and then used the size of the latter particle to calculate the nebulization efficiency [1].

Data treatment generally occurred using spreadsheets, either provided by RIKILT (NL) or Colorado School of Mines (USA). These spreadsheets use a cut-off value to distinguish dissolved and particulate signals. Partner 2 used his in-house software on basis of a deconvolution approach to distinguish dissolved and particulate signals. The latter was required because of the high background values noted for Au (carry-over) by this partner which would otherwise preclude measurement of the smallest particles.

Table II-1: Settings applied by attendees

Attendee #	**2**	**6**	**7**	**9**	**10**
Instrument	Element 2	Agilent 8800	Agilent 7700	Element 2	X-series II
Type	Sector field	Triple Quad	Quadrupole	Sector Field	Quadrupole
Dwell time	1 or 5	5	3	5	5
Datapoints	10,000	100,000	20,000	30,000	4,000
Calibration	Dissolved Au	Dissolved Au	Dissolved Au	Dissolved Au	Dissolved Au
Signal discrimination	Deconvolution	cut-off	cut-off	cut-off	cut-off
nebulization efficiency	BBI 60 nm	NIST 60 nm	NA	BBI 60 nm	NA

II.3 Sample preparation

The samples with unknown concentrations as well as the 60 nm Au NP suspension used to calculated the nebulization efficiency are diluted to different extents by the partners. Finding the optimal dilution is key to sp-ICP-MS as too high particle concentrations give rise to underestimation of particles (because of multiple particle events occurring) and too high dilution lead to a statistically insignificant count. Most partners diluted suing water, but partner 2 diluted using 0.1% cysteine to reduce memory effects of dissolved Au.

II.4 Results and discussion

Size determinations

Figure II-2 shows the different size measurements on the different instruments, whereas figure II-3 shows the relative error involved with the measurements. One clear trend is that the sector field instruments were not able to measure the 250 nm particles, whereas quadrupole instruments often were. This can be explained by the higher sensitivity of the former instruments. Large nanoparticles generate large ion clouds in the plasma, but only a small portion of those is sampled in quadrupoles, whereas the much higher transmission efficiency between plasma and detector in sector field instruments implies that a large amount of ions from these particles

reaches the detector and saturates it, thus preventing detection of these particles [3]. The sector field instruments were also the only ones that could accurately determine the 10 nm particles for the same reason. Too little ions from the ion clouds generated by the 10 nm particles reach quadrupole detectors so that they cannot be distinguished from the background.

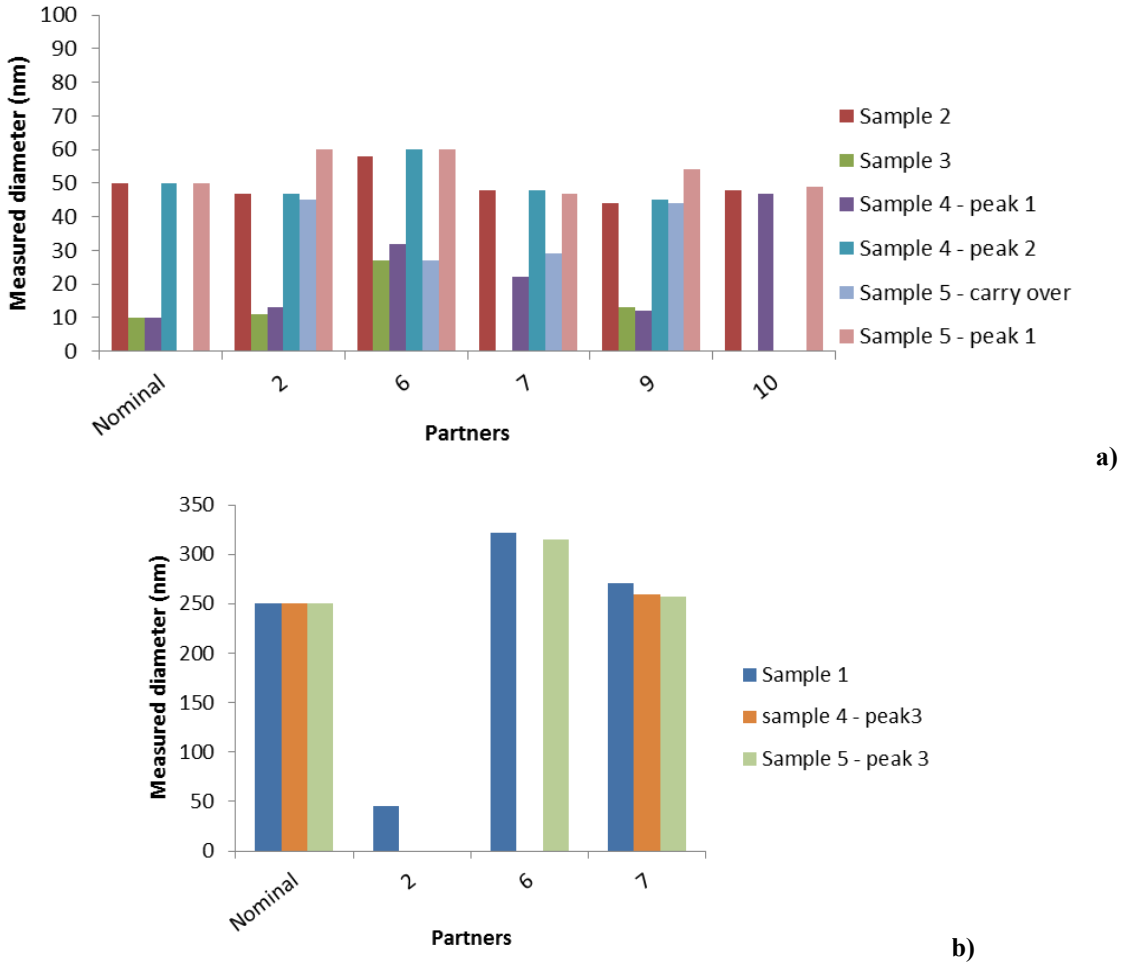

Figure II-2: a): Measured corresponding spherical diameters compared to nominal ones measured using different instruments. **b)**: shows all measurements of 250 nm nominal diameters, whereas a) show all other diameters.

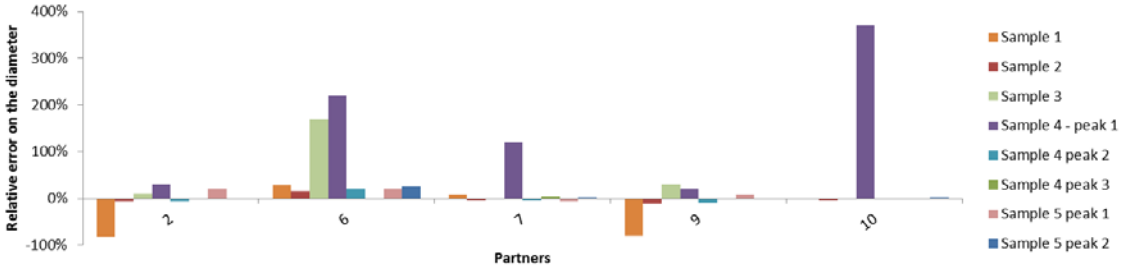

Figure II-3: Error in measured diameter relative to nominal values ((measured – nominal)/nominal values).

Figure II-3 shows large relative errors, but in most cases these are caused by the fact that no particles were detected at all or that the machines were unable to detect them or with large relative errors. The largest errors occurred with the 10 nm particles and the 250 nm particles. For instance, attendee # 1 could not detect large particles in sample 1 (250-single), but had carry-over of a few 45 nm which were detected instead. Most quadrupole partners were not able to detect 10 nm particles, but if detectable, these particles have been sized with a large error (> 10%). The 3rd root relation between corresponding spherical diameter and measured intensity is responsible for this [4]:

$$d = \sqrt[3]{\frac{((I - I_d) - I_{bkg})6qt_d\eta_e M_{w,NP}}{\pi m \rho M_{w,element}}}$$

I is the measured signal intensity (in ion counts), I_d is the dissolved level cut-off, I_{bkg} is the background concentration, ρ is the density of the nanoparticle (g m^{-3}), η_e is the nebulization efficiency, q is the sample flow rate in L s^{-1}, M_w is the molecular weight in g mol^{-1} of the nanoparticle, m is the sensitivity and t_d is the dwell time in seconds. Figure II-4 shows a typical relationship (obtained on an Element 2 for Au) between d and the difference between two consecutive I values. This difference is the bin size of the calculated particle size distribution from raw data and Figure II-4 shows how information is much denser at larger sizes, compared to smaller sizes, where small fluctuations in the number of collected ions per particle result in larger differences on the calculated diameter. Partner 6 managed to detect the small particles in sample 3 using a triple quad, but probably had a high relative error because these particles were detected very close to the size detection limit. The size detection limit was ca. 7 nm in the case of Figure II-4 where counting one or two ions results in a ca. 2 or 1 nm error on the calculated value, whereas this error is much less when detecting 10 ions per particle or more.

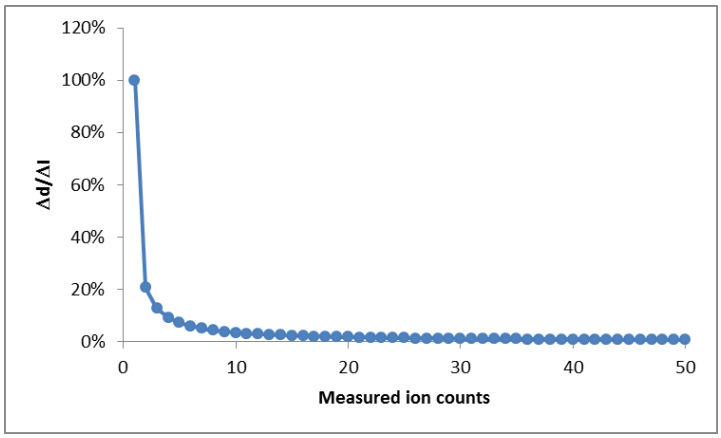

Figure II-4: A possible relation between the number of measured ion counts I_i and the difference between diameters calculated from I_{i+1} and I_i (where i > 0).

The partners with quadrupole instruments were all successful to measure the 250 nm particles in sample 3, but not always in the mixtures, especially in sample 4 where a tenfold lower concentration of 250 nm particles was added. Only attendee 7 was able to detect the larger particles in all samples, but it is unsure why this is so. Possibly 250 nm caused signals in the vicinity of the saturation threshold for other partners. Alternatively, the dilutions were too high for partners other than attendee # 7 so that only the more numerous small ones were detected in statistically significant amounts and the few detected particles were discarded as outliers. Attendee # 7 combined results from different dilutions to achieve the best results and had knowledge of the samples beforehand (attendee # 7 prepared the samples unknown to other partners for the study).

Very often, at least in conventional sp-ICP-MS, various dilutions have to be measured to avoid multiple particle events and at the same time, measure enough particles. This appears to be even more required in the case of mixtures, where multiple particle events of smaller particles can coincide with large particles thus giving a false image. FAST sp-ICP-MS, where particles are detected as Gaussian peaks, most likely will make this part of the method development and data interpretation simpler [3, 5].

Number concentrations

Collecting more data points is commonly recommended, primarily to obtain better statistics resulting in more accurate determination of the number concentration. Partner 10 with the lowest number of data points collected per sample (4,000) obtained a lower accuracy compared to other partners other than partner 2. Partner 2 had the poorest accuracy in number concentrations and most likely has made some errors as partner 9 with a very similar set-up had comparable accuracy. These observations appear to confirm that not much gain in statistical accuracy can be expected beyond 10,000 datapoints [2].

The accuracy of number concentrations for detectable particles is somewhat poorer relative to the accuracy of size determinations, but still superior compared with other methods that either could not determine this metric or even less accurately. sp-ICP-MS appears as the only method that could provide reasonable estimates of particle numbers, even in polydisperse samples, as long as the particles were detectable. It must also be stated that the nominal concentrations are not necessarily the most accurate ones as nanoparticles tend to stick to glass walls over time thus the number concentrations in suspension decrease.

Further improved accuracy can possibly be obtained. When dissolved ions pass the spray chamber with the sample, a fraction is lost to waste together with the largest droplets. More dissolved ions are lost when travelling from the plasma to the detector. The first lost fraction can be calculated using the so called nebulization efficiency, whereas the second fraction can be calculated using the so called transport efficiency. Only the nebulization efficiency is relevant to calculate the number concentration from the number of peaks because a fraction of the particles are lost, but when they make it into the plasma, they will generate peaks in the detector, even if they lose some ions between plasma and detector. Only the transport efficiency is relevant for the size, because particles do not lose Au ions during transport through the spray chamber. Dissolved ions are lost at both stages, though, so the slope of the calibration curve of measured intensity of dissolved Au vs. known concentrations is proportional to both nebulisation AND transport efficiency. There are two ways to calculate efficiencies from 60 nm Au NIST particles: using the certified size or the (non-certified) number concentration. Using this information results in estimates of respectively the transport efficiency OR the nebulization efficiency, even though this is rarely stated in literature. The counterpart efficiency is only obtained by using the sensitivity (obtained from dissolved calibration), but possibly this results in less accurate values and direct determination may be preferable.

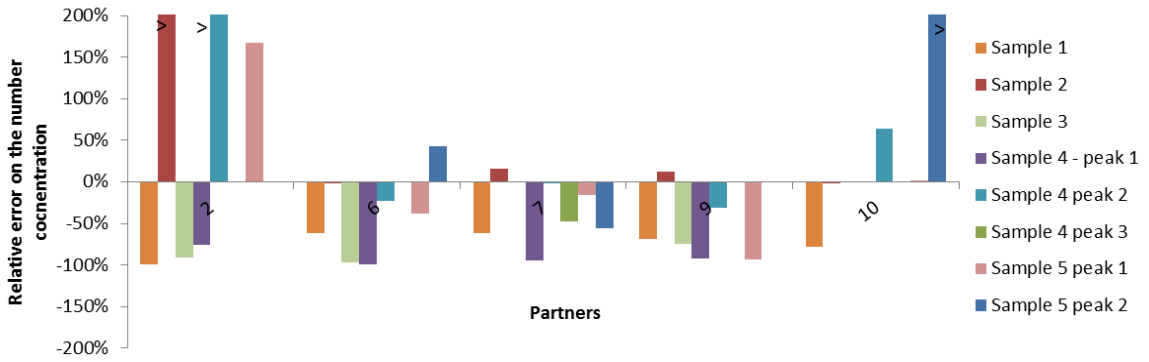

Figure II-5: Error in measured number concentration relative to nominal values ((measured – nominal)/nominal values). The symbol ">" means that the values are larger than the 200 % limit of the graph.

Another source of uncertainty is the difference between nominal and effective dwell times. Setting the instrument at a nominal dwell time of e.g. 1 ms can result in cps values of e.g. 992 cps. One ion arriving at the detector in a dwell should result in 1000 cps, which means that the effective dwell time is 1.00807 ms. Size results are more robust, because of the 3rd root [6], to such uncertainties compared to number calculations that are proportional to dwell times and errors in nebulization efficiencies. These sources of uncertainty need investigation.

Concentration range

Given the broad concentration range used and the accuracy obtained by partners other than 2 or 9, sp-ICP-MS is relatively well suited to determine number concentrations. However, the dynamic range is limited over ca. 2.5 orders of magnitude and most often, a dilution series has to be made to minimize artefacts arising from multiple particle events and/or false positives [4].

Polydispersity

By and large, sp-ICP-MS handled polydispersity well relative to methods such as DLS or NTA. The size resolution varies in the way shown in figure II-4 [6], but this cannot be deduced from the present data because the size resolution is still much better than the size differences of the particles at hand.

Many of the differences in approach stem from different instruments. This has implications on the minimal dwell time that can be used. However, using a very short dwell time is not always recommendable. In fact, 5 ms [2] or 10 ms [3] have been suggested as optimum dwell times in conventional ICP-MS where both multiple and incomplete particle events are minimized. Another, more serious implication is the large difference in sensitivity resulting in differences in both lower and upper size detection limits.

A range of dilutions should be measured so that a measurable number concentration occurs always, albeit in a different dilution. The correct number concentration is found in that range where dilution does no longer result in a reduction of multiple particle events and thus also not in an increase of the total calculated number concentration. This calculation should be done for different size ranges, because the artefact is dependent on the number concentrations that differ amongst different particles in the sample. Note that this artefact will be greatly reduced in the future when FAST sp-ICP-MS becomes more common.

Further data treatment can occur using available spreadsheets, except small nanoparticles close to the detection limit. Partner 2 has been working on software to accommodate the deconvolution method for signal discrimination [4]. Although this approach has to be validated more, it can be used for small particles.

II.5 EU definition

Given that sp-ICP-MS can determine both size and number concentration relatively accurately, it is in principle and provided that the nanomaterial is in an aqueous dispersed form, suitable for testing the EU nano definition. However, it does fail when nanoparticles are below or above the size limits of the instrument used. This may prove serious if numerous undetectably small particles are present in a sample in which there are otherwise only some large particles. The size limit is a problem from which all methods other than TEM suffer, but sp-ICP-MS is the only technique which could provide number concentrations routinely. Efforts should therefore continue to reduce the lower size limits of sp-ICP-MS whereas higher size limits can be attained by reducing the sensitivity of the instruments [3].

References:

[1] H. E. Pace *et al.*, Determining Transport Efficiency for the Purpose of Counting and Sizing Nanoparticles via Single Particle Inductively Coupled Plasma Mass Spectrometry. *Analytical Chemistry* 2011, **83**, 9361-9369.

[2] J. Tuoriniemi, G. Cornelis, M. Hassellöv, Size discrimination and detection capabilities of single-particle ICP-MS for environmental analysis of silver nanoparticles. *Analytical Chemistry* 2012, **29**, 743-752.

[3] J. Liu, K. Murphy, R. I. MacCuspie, M. R. Winchester, Capabilities of Single Particle Inductively Coupled Plasma Mass Spectrometry for the Size Measurement of Nanoparticles: A Case Study on Gold Nanoparticles. *Analytical Chemistry* 2014, **86**, 3405-3414.

[4] G. Cornelis, M. Hassellov, A signal deconvolution method to discriminate smaller nanoparticles in single particle ICP-MS. *Journal of Analytical Atomic Spectrometry* 2014, **29**, 134-144.

[5] M. D. Montano, H. R. Badiei, S. Bazargan, J. F. Ranville, Improvements in the detection and characterization of engineered nanoparticles using spICP-MS with microsecond dwell times. *Environmental Science: Nano* 2014, **1**, 338-346.

[6] J. Tuoriniemi, G. Cornelis, M. Hassellöv, Improving Accuracy of Single particle ICPMS for Measurement of Size Distributions and Number Concentrations of Nanoparticles by Determining Analyte Partitioning during Nebulisation. *Journal of Analytical Atomic Spectrometry* 2014, **29**, 743-752.

III DLS

III.1 Theoretical background of DLS

Dynamic Light Scattering (DLS) is a technique used for the measurement of nanoparticles size in suspension. The technique measures brownian motion (which is the random movement of particles due to bombardment by the solvent molecules that surround them) of the particles. The instrument is measuring the light scattered from a laser that passes through a colloidal suspension and by analyzing the fluctuation of the scattered light intensity as a function of time, the hydrodynamic size of the particle and particle agglomerates can be determined (using appropriate algorithm and Stokes-Einstein equation). Since large particles diffuse slower than smaller particles and the DLS measures the time dependence of the scattered light to generate a correlation function that then can be mathematically linked to particle size (as depicted in figure III-1).

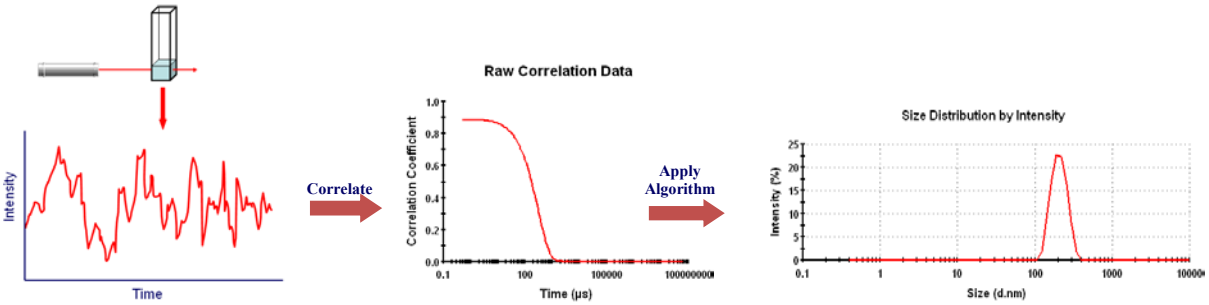

Figure III-1: Raw data transformation upon scattering experiment into particle size-distribution.

The hydrodynamic diameter is the diameter of the particle plus the ligands, ions or molecules that are associated with the surface and travel with the particle in suspension. This is way the particle appears larger to the instrument in comparison to TEM.

They are few major drawbacks to this technique; first, calculation of the hydrodynamic diameter, which is obtained based on the Stokes-Einstein equation, based on a diameter of a sphere (which may not be the case for all nanoparticles). The hydrodynamic size can also be affected by the surface structures, as well as the concentration, pH and the type of ions in the medium.

DLS produces highly reproducible and reliable measurements for monodisperse nanoparticles (usually with diameters higher than 20 nm). However, using DLS to identify the presence of multiple monodisperse nanoparticle size populations is difficult due to the high dependency of the scattering intensity on NP size. The presence of larger particles will dominate the light scattering signal and mask the presence of smaller particles (e.g. scattering intensity of a 50 nm particle is 10^6 times higher than that of a 5 nm particle). In addition, the mathematical algorithm used to analyze the autocorrelation function can lead to uncertainties in data interpretation.

III.2 Participants and analytical measures

6 attendees applied DLS for analyzing the samples (#3, #4, #5, #9, #10, #12).

Table III-1: DLS parameters

Attendee #	3	4	5	9	10	12
Instrument	Malvern	Malvern	Malvern	Malvern	Malvern	Malvern
Model applied	Volume and Number	Intensity	Intensity	Intensity	Volume	Number
Refractive Index and absorption	Polystyrene Latex & Au NPs		Au NPs	Au NPs	Polystyrene Latex	Polystyrene Latex & Au NPs

III.3 Sample preparation

Depending on the attendee and sample, the samples were measured as obtained or diluted with MilliQ water (dilution factors 1:5 – 1:20). Attendee 3 sonicated the sample for 3 min and attendee 10 sonicated the sample for 10 min prior measurement. The other attendees did not apply ultrasonication.

III.4 Results and discussion

The results obtained by the attendees are shown in table III-2.

Table III-2: Particle diameter obtained by DLS by attendees

Attendee #	3	4	5	9	10	12	STD	Real
sample	Diam. [nm]	Diam. [nm]	Diam. [nm]	Diam. [nm]	Diam. [nm]	Diam. [nm]	Diam. [nm]	Diam. [nm]
1	217	630	206	302	268	178	168	250
2	34	48	37	58	44	48	9	50
3	10	Nd	9	13	10	16	3	10
4	32	73	35	62	47	61	16 (for 50nm)	250/50/10
5	55/352	234	202	307/54	304	186	-	250/50
6	Blank	Blank	Blank	Blank	Blank	Blank	Blank	Blank

Since the DLS measures the hydrodynamic diameter of the nanoparticle it is expected that the diameters results will be larger than their actual size. But looking at the results, first of the standards alone (samples 1-3) reveals diversity of sizes, some smaller and some larger from the original nanoparticle size. This is more pronounced at the 250 nm (with STD is 168 nm) nanoparticle standard (sample number 1) while for the smaller sized Au NP (50 and 10nm – samples 2 and 3) the differences are less dramatic (SDT of 9 and 3 respectively). Looking at the unknown samples (sample 4 and 5) we got the same trend of diversity in diameters.

On the other hand most of the groups were able to find only one AuNP population in sample number 4 which contains all 3 Au NP diameters and only 2 groups where able to find the 2 AuNP populations which were in sample number 5 (the other groups found only the higher diameter AuNP – 250 nm).

The differences between the results are mostly due to differences in the measurements parameters. These were differences in measurement temperature, differences in RI (refractive index) and absorbance and the chosen distribution (intensity, volume or number; Table III-1) that was presented as the result.

Since large particles will dominate the light scattering signal and mask the presence of the smaller particles, the DLS technique exhibits problems discriminating between different NP size populations. These issues are reflected in the measurement results of the two mixtures. In sample number 4 which contains 3 different sizes of AuNP the DLS can only detect one size (the 50nm). And in sample number 5, most of the groups were able to detect only the 250 nm AuNP.

Although DLS is simple to use and the sample preparation is easy (either no sample preparation or dilution and/or sonication) and although it is a common instrument, it cannot be a reliable method for the identification of AuNP size distributions in unknown (or real) samples. Since the result were not of satisfying accuracy even when standards and standard mixtures were measured (the instrument could not find all of the different sized NP populations), detection of NP of unknown sizes and in different media must be considered not to be reliable. An *a priori* knowledge of the density and refractive index, which is required to calculate volume and number densities and to estimate the NP diameters, is not always given. Measurement of NPs in polydisperse samples in the presence of larger (nano)particles (and/or in the presence of other interfering substances) is very problematic since the scattering of the larger particles masks the scattering signals from the smaller particles, as also observed for the polydisperse samples in the ICS. This leads to false negatives or underestimation of the concentration of the smaller (nano)particles present in the sample. Measurement of small diameter NPs (less than 20 nm) is also very problematic since high concentrations are needed to achieve a signal of sufficient intensity for quantification.

To conclude, DLS is not a reliable methodology for the analysis of nanoparticle mixtures containing different sizes, given the fact that fractions smaller than 10 nm or small number-concentration in the sample are not detectable with high accuracy. DLS can only provide additional, complementary information along with further techniques.

III.5 EU Definition

Since the EU definition requires that smaller NPs can be quantified in the presence of larger ones, DLS cannot be used reliably to decide whether a material is nano or not based on the EU definition for the reasons stated above (masking effects, bias for the bigger particles, broad size distribution (a large PDI) due to other components in the sample, particle less than 20 nm cannot be detected). Hence, any attempt to rely only on the DLS to check EU criteria is not possible.

References:

[1] J. Lim *et al.*, Characterization of magnetic nanoparticles by dynamic light scattering. *Nano Review* 2013, **8**, 381.

[2] H.E. Pac *et al.*, Single particle induction couple plasma –mass spectrometry: A performance evaluation and method comparison in the determination of nanoparticle size. *Environmental Science and Technology* 2012, **46**, 12272.

IV Imaging evaluation AFM/TEM

IV.1 Theoretical background of AFM/TEM

After deposition of the particles on a suitable substrate (AFM: flat surface (e.g. freshly cleaved mica), TEM: electron transparent thin film (e.g. Cu grid coated with a thin layer of carbon (commonly referred to as TEM grid)), SEM: flat surface (e.g. polycarbonate filter or TEM grid)) the sample can be imaged using different detection methods. In the AFM, the tip of a very sharp needle is scanned over the sample surface. Thereby, the tip of the needle very closely follows the surface of the sample and thus accurately records the topography of the sample. Particles therefore appear as individual 'mountains' (AFM images contain 3D information (x,y,z)) on a flat plain (sample substrate) [1]. In SEM, a focused electron probe is scanned over the sample and various signals caused by the interaction of the electron probe with the sample are recorded at every position. Most commonly, secondary electrons (SE) are used for high resolution images, but also transmitted electrons can be used for image formation [2]. Similar to the AFM images, SEM-SE images represent the topography of the sample surface, although the image contains no true 3D information. In the TEM, the sample is irradiated with a parallel electron beam and the transmitted electrons are recorded by a CCD camera. In the TEM image, particles therefore appear as dark spots on a bright background [3].

IV.2 Participants and analytical measures

Four partners used imaging techniques (3 x TEM, 1 x AFM) to investigate the 5 samples (table IV-1). The particle size distribution was derived from recorded images using image analysis tools. Some partners 'manually' measured the particle size and others used largely automated analysis scripts. Therefore, the number of particles included to derive a particle size distribution varied over more than one order of magnitude. It was agreed to report the minimum Feret diameter, but this parameter may be difficult to assess by manual measurements. However, as the particles were expected to be close to spherical, the difference between the different diameters is expected to be rather small.

IV.3 Sample preparation

Attendee # 3:
Applied technique: AFM
Samples were store at 4°C until they were analyzed. Before the imaging with AFM the samples were shaken. The drop deposition technique of sample preparation was used, a 5 µL of sample was pipetted directly onto freshly cleaved mica surface and were allowed to dry for acc 30 min in an enclosed Petri dish before imaging.

Attendee # 8:
Applied technique: TEM
The Au stocks were kept in the fridge from the moment that they arrived. Au stocks were diluted (sample 1: 1:5, sample 2: 1:1000, sample 3: 1:100, sample 4: 1:100, sample 5: 1:10) using doubly deionized (DDI) water. Suspensions were bath sonicated for 5 minutes before centrifugation. Diluted suspensions (1 mL) were centrifuged onto carbon coated Cu grids (1h, 14000 x g). TEM grids were removed from the centrifugation vials and washed 3 times by dipping the grids in a drop of DDI water.

Attendee # 9:
Applied technique: TEM
For samples 1 and 5, no dilution was made. Samples 2, 3 and 4 were diluted by 10 with MilliQ water (100 µL of sample in 1 mL of water). 5 µL of each samples were deposited on ionized-grids

Attendee # 10:
Applied technique: TEM
The samples were sonicated for 20 min and then One 5 micro-liter drop of the suspension (no dilution) was placed on the grid and blotted by filter paper after one minute.

IV.4 Results and discussion

All results are given in Table IV-1 and will be discussed in the following sections.

Table IV-1: Summary of the particle size distributions (average minimum Feret diameter), standard deviation (1 σ) and number of particles analyzed per particle mode

Attendee #	**Exp. size**	**3** [3,5]	**8** [1,2,4]	**9** [3,4]	**10** [3,4]
Sample	**Diameter (nm)**				
1	*250*	200 ± 19	240 ± 72 / 494	*n.d.*	254±28 / 99
2	*50*	17 ± 20	51 ± 25 / 119	46 ± 5.0 / 11	44±4 / 227
3	*9.5*	12 ± 8.9	8.0 ± 1.5 / 939	8.2 ± 0.7 / 11	8.0±1 /146
4	*9.5*	13 ± 9.7	9.1 ± 6.0 / 438	9.3 ± 0.8 / 19	8.0±1/136
	50	33	49 ± 22 / 150	48 ± 3.4 / 28	45±4/16
	250			n.d	269±24 /11
5	*50*	44 ± 40	45 ± 5.7 / 103	49 ± 5.0 / 14	51±3/12
	250	200 ± 40	250 ± 54 / 575	290 ± 26 / 24	292±24/28

[1]: Average particle sizes and standard deviations refer a normal distribution that was fitted to the experimental data.
[2]: automated measurements
[3]: manual measurements
[4]: TEM
[5]: AFM

For the medium (50 nm) and the smallest (10 nm) particle sizes, the majority of the results were in good agreement with the nominal size values (mostly within 1 standard deviation). For the monomodal suspensions, the largest absolute deviations occurred for the largest particle sizes (250 nm). One attendee could not detect the 250 nm Au NPs at all. Similar observations were also made for the polymodal size distributions and also the largest particle mode (expected value 250 nm) was either not detected or the values deviated substantially from the nominal values. Results from AFM measurements tended to underestimate the particle size, which may be

related to the fact that in the AFM measurements, the height is recorded, which may not exactly correspond to the nominal value reported by the manufacturer.

The most significant differences in absolute particles sizes (compared to the nominal diameters) were observed for the largest fractions (250 nm). A possible reason for these differences may be the particle shape which increasingly deviated from the perfect sphere with increasing particle diameter. This may have led to a larger error in manual measurements and may have introduced an operator bias. The automated image analysis resulted in a considerable standard deviation (240 nm ± 72 nm / 494 particles) which may indicate a broader size distribution than for the smaller particles. Also this fact may have introduced an operator bias when only a small number of particles were analyzed.

The most critical part in the application of imaging technique to derive quantitative size information is the sample preparation. This is particularly challenging when different particle sizes (modes) occur at very different number concentrations. Optimizing the sample preparation for one particle mode may lead to an unsuitable (too much or too few) number of particles of another particle mode on the sample carrier. This was for example the case in sample 4, which contained particles of all three modes (10 nm, 50 nm, 250 nm). In this sample, the number of 250 nm particles was almost 5 orders of magnitudes lower than the 10 nm particles.
Although the size of the particles can reliably be determined using imaging techniques, a big challenge is the determination of the absolute particle number concentration. Frequently used sample preparation techniques include the 'drop deposition' - (a drop of suspension is air dried on the sample carrier) and the 'adsorption' - (a sample carrier is placed on a drop of suspension and the particle transported to the carrier surface by diffusion) techniques. In the first case, drying artefact generally result in an uneven distribution of the particles on the sample carrier and in the latter case, the suspension volume from which particles are deposited on the sample carrier is ill defined. Thus, the quantification of the particles number concentration based on these sample preparation methods is not feasible. A possible solution to this is to directly centrifuge particles from well-defined suspension volumes on sample carrier. This approach was tested by one lab, however, an even distribution of the particles on the sample carriers was not obtained and particles mostly occurred in clusters of a several tens of primary particles leading to an uneven particle distribution on the sample carrier (Figure IV-1 and IV-2). The reason for this is currently unknown, but may have been related to the surface properties of the sample carrier. Further experiments will address this issue by adapting the surface of the sample carrier to the surface properties of the particles. Thus, none of the microscopy labs were able to deliver any particle number concentration.

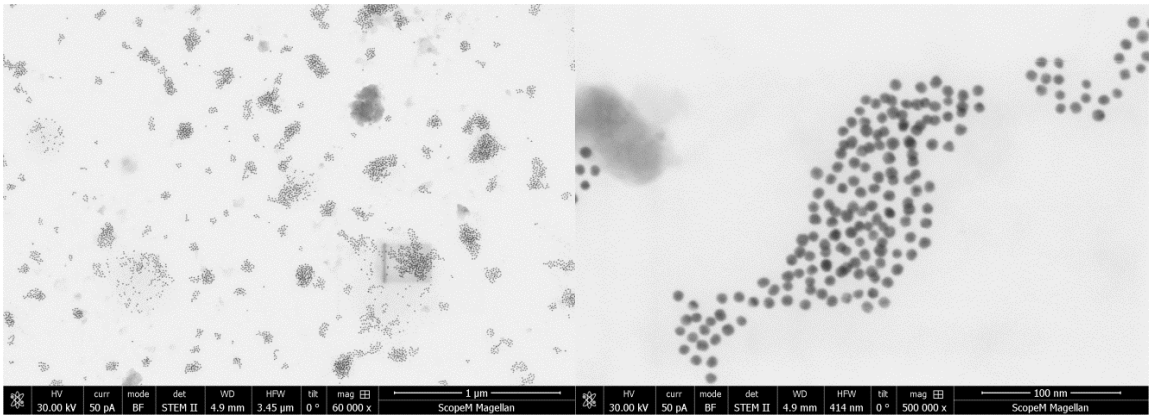

Figure IV-1 and IV-2: Cluster formation of Au-NPs (10 nm) on the sample carrier.

The big advantage of imaging techniques are that the results (derived from image analysis) are directly number based as required by the current recommendation of the EU definition and therefore do not require any conversion algorithms (from mass/volume to size).

Results from imaging techniques (in combination with image analysis) are directly based on particle numbers. Thus, also polydisperse and polymodal samples can be investigated as larger fractions do not negatively interfere with smaller particles (as for example in light scattering techniques). However, if the number concentrations of different particle modes in a suspension are very different (as for example in sample 4) then the analysis of both particle modes may require two separately prepared samples (one dedicated for the smaller and one for the larger particle mode).

IV.5 EU definition

Imaging techniques appear to be suitable for a decision "Nano: Yes/No" in terms of the EU Definition, if the sample preparation is adequate. However, it first has to be demonstrated that the sample (used for imaging) is 'representative'.

Thus, in case of Au NPs and based on the ICS results obtained with imaging techniques, the EU definition seems to be suitable and applicable. However, for the imaging techniques, guidelines concerning sample preparation and data evaluation (which diameter is reported) and how is the particle size distributions are reported (histogram vs. fitted distributions) are necessary.

References:

[1] E. Meyer, H.J. Hug and R. Bennewitz, Scanning Probe Microscopy: The Lab on a Tip. *Springer Science & Business Media* 2013.

[2] J.I. Goldstein, D.E. Newbury, P. Echlin, D.C. Joy, C.E. Lyman, E. Lifshin, L. Sawyer and J.R. Michael, Scanning Electron Microscopy and X-ray Microanalysis. *Boston, MA, Springer US* 2013.

[3] D.B. Williams and C.B. Carter, Transmission Electron Microscopy: A Textbook for Materials Science. *Springer Science & Business Media* 2009.

V Total Au concertation ICP-MS/-OES

V.1 Theoretical background of ICP-MS/OES

Inductively Coupled Plasma-Mass Spectrometry/-Optical Emission Spectrometry (ICP-MS/ICP-OES) [1] are powerful tools allowing the detection and quantification of multiple chemical elements in a large variety of man made products, geological, environmental and biological samples [2]. For example, it is currently applied to the multi-elementary analysis in surface waters [3], soils and sediments [4] as well as petroleum [5] or biological fluids [6]. The principle of ICP techniques is the introduction of aerosol samples into an argon plasma. The plasma dries the aerosol, dissociates the molecules (atomization), and then forms charged ions by removing electrons from the atoms. These ions are directed into a mass filtering device known as the mass spectrometer (ICP-MS), which allows the ion separation according to their mass-to-charge ratio (*m/z*) [7]. In addition, inductively coupled plasma produces excited atoms and ions that emit element-characteristic electromagnetic radiation. The light intensity of this emission is indicative of the concentration of the element within the sample and is measured in the optical chamber(s) (ICP-OES). Thus, ICP-MS and ICP-OES allow for the analysis of (almost) the entire periodic table.

In the frame of the test performed the ICP-MS/OES measurements were expected to give information on the total metal concentrations (here Au concentration in the 5 samples + 1 blank) of the suspensions. Further information regarding, e.g. size-distribution is not aimed at by means of this measurements.

V.2 Participants and analytical measures

Six partners (#4, #5, #7, #9, #10, #12) analyzed the samples with either ICP-OES (3 partners), ICP-MS (2 partners) or both methods (1 partner) (Tables V-1a and V-1b).

Table V-1a: ICP-OES parameters applied by attendees # 4, # 5, # 9, # 12

Attendee # **ICP-OES parameters**	**4**	**5**	**9**	**12**
type of nebulizer	zyclon, seaspray, twister glass	Crossflow	Quartz	parallel path nebulizer, Burgener Mira Mist
nebulizer gas flow [L/min]	220 kPa	0.73	0.3	0.6
auxiliary gas flow [L/min]	1.5	0.8	0.5	0.2
plasma gas flow [L/min]	15	11	12	10
RF power [W]	1350	1400	1150	1300
time of analysis per sample [min]	2.5	3	3	
wavelength monitored	242.794/208.207 nm	267.595 nm	208,209 nm	267,595 nm
Analyte	Au	Au	Au	Au
internal standard	none	Y	none	none

Table V-1b: ICP-MS parameters applied by attendees # 7, # 10, # 12

Attendee # / ICP-MS parameters	7	10	12
type of nebulizer	MicroMist	MicroMist	MicroFlow PFA
nebulizer gas flow [L/min]	0.99	1.09	1.07
He gas	-	-	5
auxiliary gas flow [L/min]	-	0.9	0.9
plasma gas flow [L/min]	15	15.02	15
RF power [W]	1550	1550	1400
dwell time [ms]	1000	200	0.3
Runs	3	3	5
Passes	1	3	1
Sweeps		100	100
time of analysis per sample [min]	7,2 sec + 18 s uptake before and after acquisition	0.5	0.44
isotopes monitored	^{197}Au	^{197} Au	^{197}Au [He-Mode]
internal standard	^{175}Lu	^{157} Gd	^{72}Ge, ^{103}Rh, ^{185}Re

Data treatment:

All partners performed data treatment based on external calibration, with standards typically ranging from 1 to 5000 µg/L for ICP-OES and from 1 to 650 µg/L for ICP-MS. Partners running ICP-MS techniques used either ^{72}Ge, ^{103}Rh, ^{185}Re, ^{175}Lu or ^{157}Gd as internal standard to correct from the instrumental mass bias drift (see Table V-2).

Table V-2: External and internal standards information used by each partner for data treatment

Attendee # / Sample	4 [µg/L]	5 [µg/L]	7 [µg/L]	9 [µg/L]	10 [µg/L]	12 [µg/L]
substracted blank	0	0	0	0	0	0
standard 1	25	500	5	1.04	25	10
standard 2	50	1000	1	5.11	50	20
standard 3	150	1500	2	10.05	75	50
standard 4	300	3000	5	52.11	100	100
standard 5	500	4000	10	102.61	150	200
standard 6	X	X	X	509.5	200	500
standard 7	X	X	X	1015.15	300	1000
standard 8	X	X	X	X	400	2000
standard 9	X	X	X	X	500	5000
standard 10	X	X	X	X	650	X
internal standard	none	Y	^{175}Lu	none	^{157}Gd	^{72}Ge, ^{103}Rh, ^{185}Re

V.3 Samples preparation

The sample preparation displays discrepancies among the partners. 3 partners performed acid-digestion in aqua regia (2/5 conc. HNO_3 + 3/5 conc. HCl) warming either with hot plate or with microwave. 1 partner diluted samples in HCl 1% and another one did both preparations. The sixth partner diluted in HNO_3 1% + HCl 3% after sonication (see Table V-3).

Table V-3: Conditions deployed for sample preparation

Attendee #	**4**	**4**	**5**	**7**	**9**	**10**	**12**
Sample preparation	Aqua regia 60°C	Dilution in 1% HCl without aqua regia	aqua regia + microwave	aqua regia + microwave	acidification with HCl 37% before dilution x10 in MilliQ	dilution x100 in 1% HNO_3 and 3% HCl after 30min sonication	aqua regia + microwave

V.4 Results and discussion

The average concentrations measured by all attendees were found from 0.4% to 26% different (generally lower) from the theoretical ones, depending on the samples (Table V-4 and Figure V-1). No discrepancy was found between ICP-OES and ICP-MS results: given the relatively high concentrations of the 5 samples distributed (56-57 mg/L), both methods can be considered efficient for their measurement, providing an adapted dilution and sample preparation.

The main differences observed between partners can reasonably be related to the sample preparation protocol. Three of the four partners (#5, #7, #12) using aqua regia for sample preparation systematically found results falling in the 5-10% range regarding the theoretical value concentrations. The fourth one (partner #4) globally obtained overestimated values (+40 to +80%), which can reasonably be attributed to the small standard range used (from 25 to 500 µg/L), leading to a probable extrapolation of results. Astonishingly, the partner #10 obtained similar results (i.e. within the 5-10% range) without using a real digestion with aqua regia, but diluting samples with HNO_3 1% and HCl 3% mixture, after a first sonication step of 30 min. Partner #9 obtained results extremely underestimated, compared to the theoretical values (globally one order of magnitude lower, see Table V-4). This partner prepared the samples with an acidification with HCl before dilution with MilliQ water to reach a HCl 1% matrix. No total acid digestion with aqua regia nor sonication were used, which may lead to only partial dissolution of the biggest AuNPs. However, partner #4 also performed such a dilution with HCl which led to results globally overestimated.

Consequently, it remains unclear to determine the exact process (aggregation, settling) which occurs when a simple acidification with subsequent dilution is used to prepare the AuNPs samples. However, it clearly appears that the use of aqua regia generally leads to similar results, which may be linked to the rate of NP dissolution. In addition, the use of sonication, supposed to break the AuNPs aggregates, allows to display results highly similar to the acid digestion ones.

Table V-4: Summary of ICP-OES and ICP-MS results obtained by each partner as well as theoretical values and averages by method

Sample	Nominal Size	Partner	4	4	5	7	9	10	12	12	Avg	Avg	Avg	Avg
		theoretical value	ICP-OES aq. reg.	ICP-OES dilution	ICP-OES	ICP-MS	ICP-OES	ICP-MS	ICP-OES	ICP-MS	all results	ICPMS	ICPOES	Aqua regia
	[nm]	[mg/L]	[mg/L]	[mg/L]	[mg/L]	[mg/L]	[mg/L]	[mg/L]	[mg/L]	[mg/L]	[mg/L]	[mg/L]	[mg/L]	[mg/L]
1	250	56.8	81.6	58.2	26.4	44.5	1.0	43.4	38.8	39.8	41.7	42.6	41.2	46.2
2	50	56.8	102.5	97.2	49.0	53.8	2.9	61.9	54.9	59.1	60.2	58.3	61.3	63.9
3	10	57.6	103.1	93.8	46.0	51.0	3.9	56.2	50.9	54.1	57.4	53.8	59.5	61.0
4	17.3 mg/L of 10 nm; 28.4 mg/L of 50n m; 11.4 mg/L of 250 nm	57.0	81.0	88.2	45.4	51.5	0.9	55.9	51.9	52.6	53.4	53.3	53.5	56.5
5	2.8 mg/L of 50 nm; 54 mg/L of 250 nm	56.8	80.1	73.7	37.5	45.9	1.3	47.2	43.9	42.1	46.5	45.1	47.3	49.9

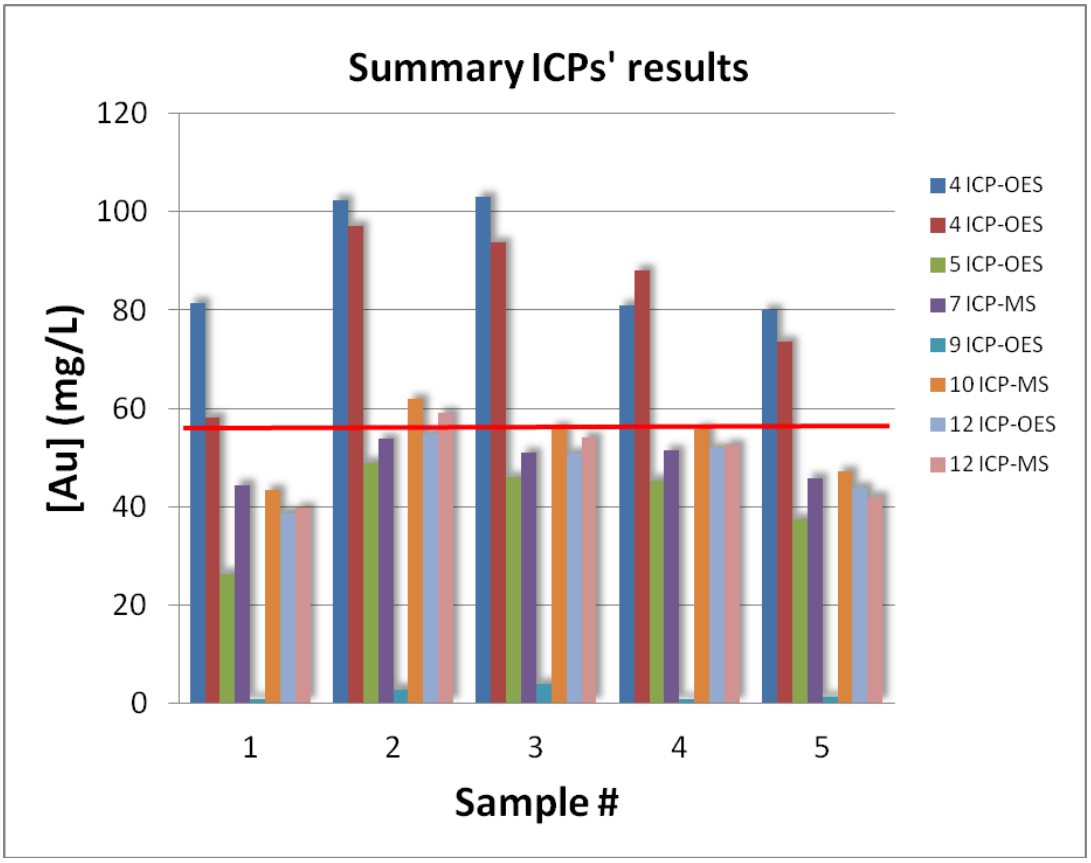

Figure V-1: Summary of Au concentrations determined by attendees applying ICP-MS and/or ICP-OES.

V.5 EU Definition

As mentioned above the information envisaged by means of ICP-MS/-OES measurements were total metal concentrations; thus, assessing whether a sample is a nanomaterial or not based on the EU definition is not possible based on the results obtained.

References:

[1] H.E. Taylor, Inductively Coupled Plasma-Mass Spectrometry: Practices and Techniques 2001.

[2] H.-E. Gabler, Applications of magnetic sector ICP-MS in geochemistry. *Journal of Geochemical Exploration* 2002, **75**, 1-15.

[3] I. Zelano, Y. Sivry, C. Quantin, A. Gelabert, M. Tharaud, D. Jouvin, E. Montarges-Pelletier, J. Garnier, R. Pichon, S. Nowak, S. Miska, O. Abollino and M.F. Benedetti, Colloids and suspended particulate matters influence on Ni availability in surface waters of impacted ultramafic systems in Brazil 2013.

[4] Y. Sivry, M. Munoz, V. Sappin-Didier, J. Riotte, L. Denaix, P. de Parseval, C. Destrigneville and B. Dupré, Multimetallic contamination from Zn-ore smelter: solid speciation and potential mobility in riverine floodbank soils of the upper Lot River (SW France). *European Journal of Mineralogy* 2010, **22**, 679-691.

[5] G. Caumette, C.-P. Lienemann, I. Merdrignac, H. Paucot, B. Bouyssiere and R. Lobinski, Sensitivity improvement in ICP MS analysis of fuels and light petroleum matrices using a microflow nebulizer and heated spray chamber sample introduction. *Talanta* 2009, **80**, 1039-1043.

[6] P.C. Kruger, L.M. Schell, A.D. Stark, A.D. and P.J. Parsons, Lanthanide distribution in human placental tissue by membrane desolvation-ICP-MS. *Journal of Analytical Atomic Spectrometry* 2010, **25**, 1298-1307.

[7] N. Jakubowski, L. Moens and F. Vanhaecke, Sector field mass spectrometers in ICP-MS. *Spectrochimica Acta Part B: Atomic Spectroscopy* 1998, **53**, 1739-1763.

VI Chronoamperometry (electrochemical method)

VI.1 Theoretical background of electrochemistry

Electrochemical methods can offer a new approach in the analysis of water samples that contain NPs. They can be used for analysis of the samples which contain electrochemically active NPs and in the same time differentiate NPs according to their composition. The approach can be used efficiently for the analysis of samples with low concentration of NPs as well as polydisperse samples. The main advantage of the method is a direct and easy performance of measurements which in the same time can be used to monitor aggregation processes of the NPs [1-5].

VI.2 Participants and analytical measures

One attendee of the ICS applied electrochemistry (#3).

Chronoamperometric measurements were conducted by application of a step potential; the current (i) is measured as a function of time (t) at a fixed potential between the working and the reference electrode. The following instrumental parameters were applied: i) applied potential of 1.0 to 1.2 V (vs. Ag/AgCl); ii) sampling or interval time was 0.0004-0.0008 s; iii) measurement duration was 1-5 s; iv) current range during measurement was 100 nA-1 μA.

All measurements were performed with Autolab PGSTAT128N potentiostat (Eco Chemie, Utrecht, Netherlands) at the GC microelectrode as working electrode, while carbon rod and Ag/AgCl served as counter and reference electrode, respectively (Fig. VI-1).

All measurements were performed in electrolyte solutions of various composition and ionic strengths. Due to rapid oxidation of the colliding Au NPs with the surface of the GC microelectrode, the short-duration current transients (spike like signals) superimposed on the diffusion limited background current were recorded (Fig. VI-1). The charge of the spike like signals was used to assess size of the NPs. After every measurement the GC microelectrode was cleaned by polishing.

VI.3 Sample preparation

Aliquots of Au NPs samples 1-5 (10-300 uL) were directly (without further pretreatment) added in the 10 mL of electrolyte solutions previously purged for 4 min. with nitrogen. $NaNO_3$, H_2SO_4 and NaCl of different ionic strengths (0.01-0.1 M) were used as electrolytes. The best responses were observed with $NaNO_3$. To avoid the sample agglomeration only 1:1 electrolytes were used ($NaNO_3$, NaCl), and due to possible complex formation with Cl^- most of the experiments were carried out in $NaNO_3$, especially at higher ionic strengths of used electrolytes. Before addition of the sample the electrolyte solution was purged with nitrogen and the blank was recorded.

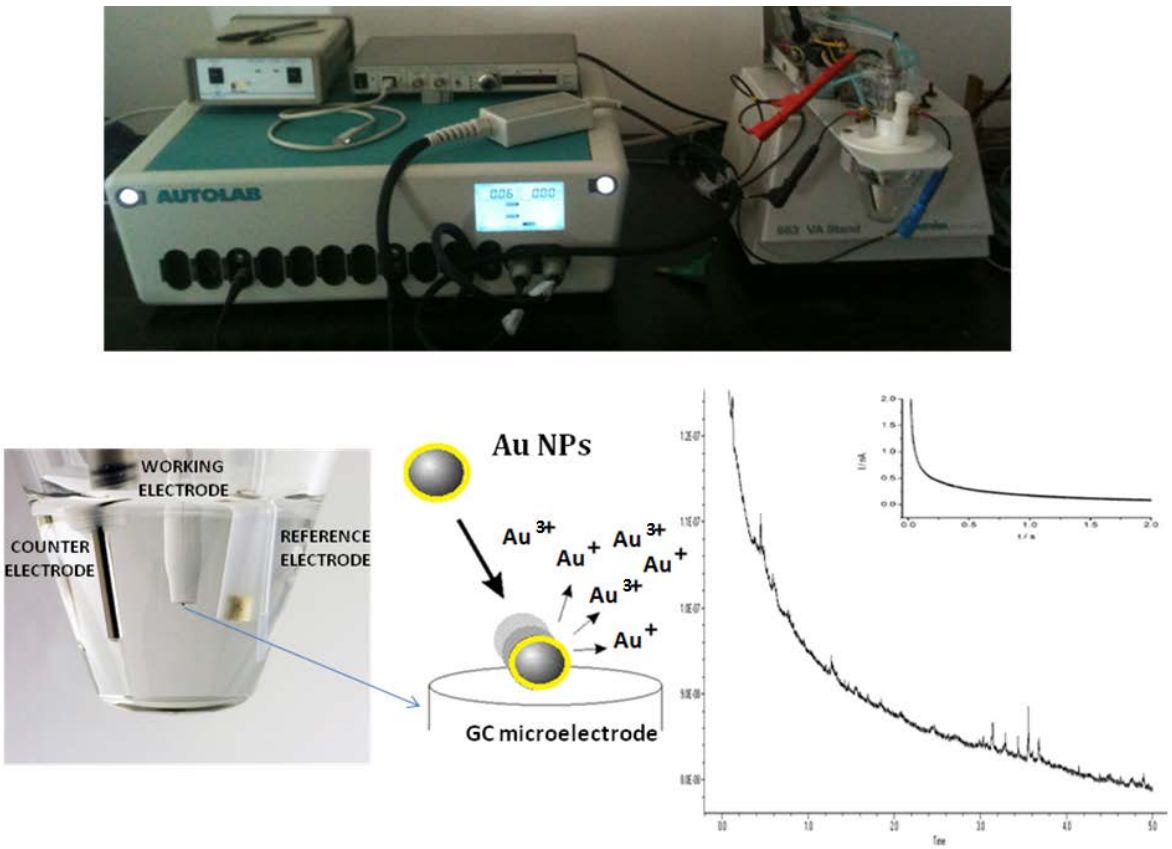

Figure VI-1: Experimental setting and schematic description of Au NPs oxidation at the GC microelectrode with chronoamperogram in the pure electrolyte (insert) and Au NPs dispersion.

VI.4 Results and discussion

Theoretical background on chronoamperometric data assessment:

Observed i-t response is a combination of two components: capacitative current related to the charging the double-layer and Faradaic current related to the electron transfer reaction, e.g. sharp current transients due to Faradaic charge transfer during contact of the NPs with the GC microelectrode [1-5].
In case of the Au NPs which interact with the GC microelectrode, collision is accompanied with oxidation of the colliding Au NPs [1].

$Au + H_2O \rightarrow Au^{d+}OH^{d-} + H^+ + e^-$
$2Au + 3H_2O \rightarrow 2AuO_2 + 2H^+ + 2e^-$

During oxidation of Au NPs the transient current signals superimposed on the chronoamperometric i-t curve are observed. All chronoamperometric curves were analyzed in the same way to eliminate possible influence of detector noise. The charge of the spike like signals was used to assess the size of the NPs. Assuming that the Au NPs are spherical and that during the oxidation of Au NPs the 1.9±0.1 electrons are transferred per Au atom [1] the size was calculated using the equations Eq VI-1 and Eq VI-2 [2,3]:

$$r = \sqrt[3]{\frac{3A_r N_m}{4\pi N_A \rho}};\ N_M = Q/ze \quad \text{(Eq VI-1)} \quad \text{and} \quad r = \sqrt[3]{\frac{3A_r Q}{4z\pi F\rho}} \quad \text{(Eq VI-2)}$$

where *Ar* is relative mass of gold atom, *Q* is a charge of observed spike like signal, *F* is the Faraday constant, N_A is the Avogadro number, ρ is the density of gold, and z is the number of electrons exchanged during oxidation. The size obtained with Eq VI-1 and Eq VI-2 showed insignificant variation in sizes.

Intercomparison results:

Fig. VI-2 shows the chronoamperogram for the Sample 2 where the charge of the recorded current transients ranged from the 2.18×10^{-12} C to 6.82×10^{-12} C. Difference in the calculated size of the Au NPs and their frequency, measured in several runs (as illustrated in Fig. VI-2) is shown in Fig. VI-3. NPs sizes are calculated from the recorded spikes i.e. charges presented in Fig. VI-2 by Eq VI-1.

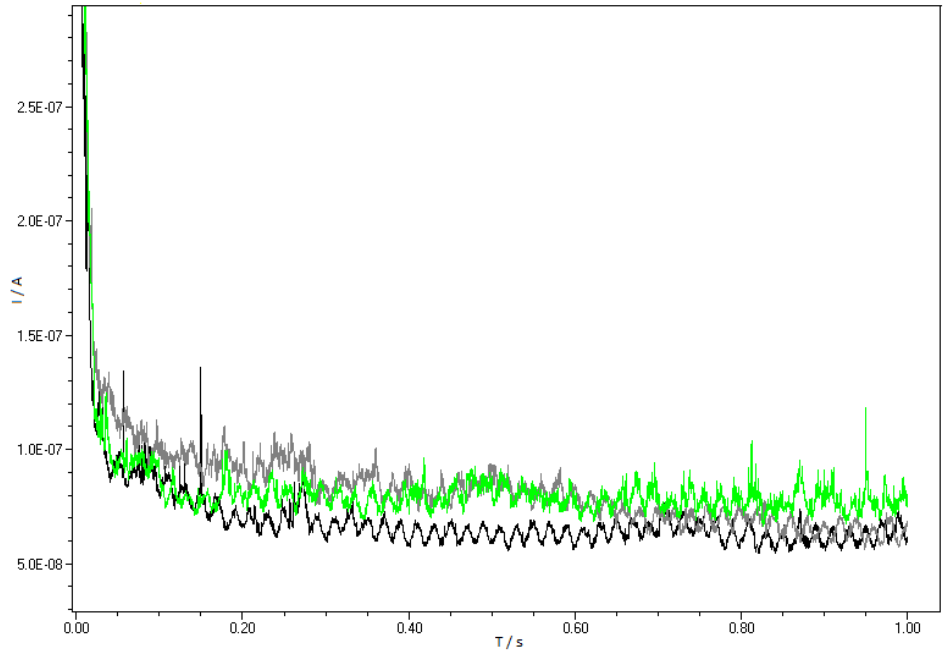

Figure VI-2: Repeated measurements of sample 2 in 0.1 M $NaNO_3$ at 1.0 V (vs. Ag/AgCl); electrode was polished before each measurement.

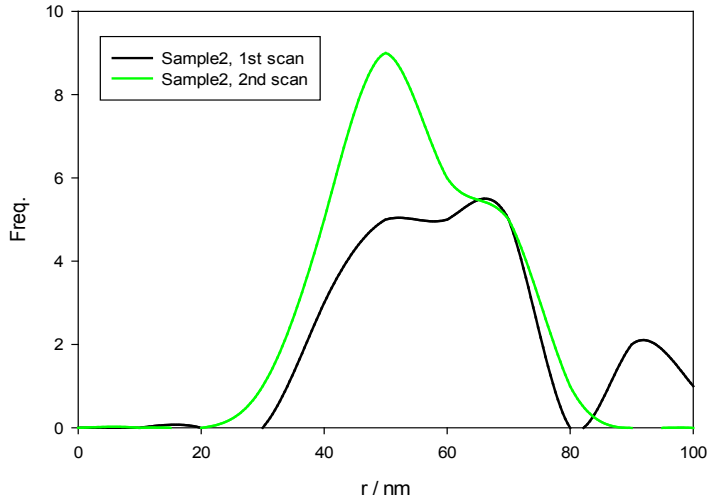

Figure VI-3: Size distribution of the Au NPs in Sample 2 calculated from the curves presented in Fig. VI-2.

It appears that chronoamperometry can be used as a sizing technique for the Au NPs. Analysis of the recorded spikes-charges in sample 2 gave radii of 50 nm (Fig. VI-3), what indicates agglomeration of the Au NPs upon addition to the electrolyte solution or in the original Sample 2. The technique is sensitive to the different concentration of the Au NPs and it appears that it is beneficial for monitoring of agglomeration processes in the samples (Fig. VI-4) [1-4].

The frequency of the spike signals, which is believed to carry information on the concentration of the NPs, varies significantly in dependence of the experimental conditions (e.g. electrolyte composition, ionic strength, microelectrode surface,…); thus, further investigation and development of the experimental procedure is necessary.

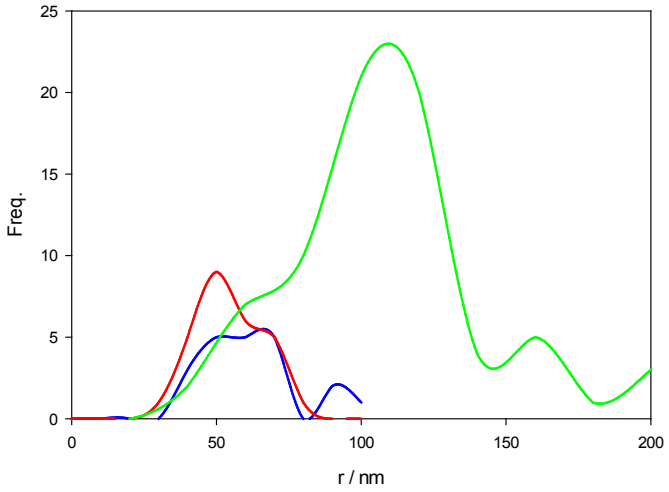

Figure VI-4: Radii vs. frequency of the spikes recorded for Au NPs sample 2 at 1.0 V (vs. Ag/AgCl) in different experimental conditions: blue – 0.1 M $NaNO_3$ (50 µL sample 2 / 10 mL), red -the same as in blue, but on polished GC surface in the second scan, and green - 0.1 M H_2SO_4 (100 µL sample 2 / 10mL).

Although in the analyzed samples some spikes were recorded, a detail quantitative analysis of the recorded chronoamperometric curves is still lacking due to problems that arose during the measurements:

- Lack of the reproducibility of the measurements,
- Charge of the observed current transients was similar to values reported in the literature for the Au NPs in the size range from 10 – 200 nm, but the background current was much higher than expected for the GC microelectrode,
- Problem with obtaining reproducible microelectrode surface,
- Strict experimental procedure for the chronoamperometric measurements (working electrode potential, sampling duration, sample time, current range),
- Unsatisfactory reproducibility influenced uncertainties in the calibration plots,
- Further work is in process to overcome noted problems in the chronoamperometric measurements of Au NPs.

VI.5 EU Definition

Given the fact that chronoamperometry can determine size of the Au NPs based on the charged passed during the contact between the Au NPs and the electrode surface it can be used as a qualitative measure of the Au NPs present in the sample. There is still no information about upper size limit in the detection of the Au NPs with chronoamperometry. Our chronometric study on the metal sulfide NPs indicate that the method fails to detect larger particles (> 200 nm) leading to wrong conclusions whether the dispersion is a nanomaterial or not. The other main obstacle is that chronoamperometric measurements are still lacking on information on the Au NPs concentration.
Considering the inability to detect all particles sizes in sample and absence on the number-based concentration data of the Au NPs the method is not suitable for sample assessment with regard to the EU definition.

References:

[1] Y. Zhou, N.V. Rees, J. Pillay, R. Tshikhudo, S. Vilakazi and R.G. Compton, Gold nanoparticles show electroactivity: counting and sorting nanoparticles upon impact with electrodes. *Chem. Commun.* 2011, **48**, 224-227.

[2] Y.G. Zhou, N.V. Rees and R.G. Compton, The Electrochemical Detection and Characterization of Silver Nanoparticles in Aqueous Solution. *Angewandte Cemie* 2011, **50**, 19-21.

[3] J. Tschulik, K. Stuart, E.J.E. Jurkscha, K. Omanović, D. Uhlemann, M. Crossley and G. Compton, Get More Out of Your Data: A New Approach to Agglomeration and Aggregation Studies Using Nanoparticle Impact Experiments. *Chemistry Open* 2013, **2**, 69-75.

[4] E. Bura-Nakić, M. Marguš, D. Jurašin, I. Milanović and I. Ciglenečki-Jušić, Chronoamperometric study of elemental sulphur (S) nanoparticles (NPs) in NaCl water solution: new methodology for S NPs sizing and detection. *Geochem. Trans.* 2015, **16**, 1-9.

[5] E. Bura-Nakić, M. Marguš, D. Jurašin, I. Milanović and I. Ciglenečki-Jušić, The development of elctrochemical methods for determining nanoparticles in the environment. Part II: chronoamperometric study of FeS in sodium chloridee solution. *Environ. Chem.* 2014, **2**, 187-195.

VII Hydrodynamic Chromatography / Field-flow fractionation

VII.1 Theoretical background of HDC/FFF

Detailed theoretical considerations are out of the scope of this report and the reader is referred to the respective literature. Hence, the theoretical background of the respective techniques is highlighted just briefly:

HDC

Hydrodynamic chromatography (HDC) can be performed using a capillary or a column packed with uniform microspheres. Interestingly, the model used for the capillary can be applied straightforwardly to the case of a packed column with excellent confidence with measurements [1]. This simple model is described in figure VII-1. In a cylindrical tube a Poiseuille flow transports particles at different velocities. Because of steric exclusion, large particles can access only to the central region of the tube where the parabolic flow is the strongest and thus the average velocity the highest. Smaller particles can access to the region near to the wall; their average velocity is therefore lower. Thus, large particles will tend to elute faster than small particles and all particles will elute faster than or as fast as the eluent.

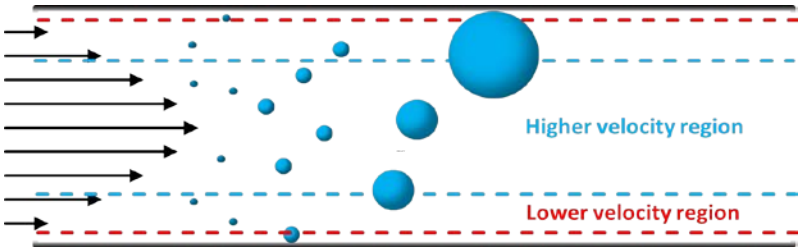

Figure VII-1: Schematic description of the separation mechanism in HDC.

The model is based on the following hypotheses [2]:

- The flow is laminar. There is hence an upper limit for the flow velocity and the pressure for a given chromatographic system.
- Particles efficiently sample the whole velocity profile. This is the case for colloidal particles as they have high diffusion coefficients, provided that the elution time is long enough.
- Effects of affinity or collision of the particles with themselves or the wall are negligible. This is correct when the particle concentration in the sample is small enough and when the electrostatic and chemical forces between the wall and the particles are weak.
- Particles are spherical or similar to spheres.
- The packed column can be approximated by parallel tubes with inner radius.

This simple model successfully described the elution of spherical particles in HDC in most cases encountered in the literature and with diverse types of particles [1, 3, 4, 5].

FFF

Field-flow fractionation (FFF), is a flow-based fractionation methodology, which was invented and theoretically described by John Calvin Giddings in 1966 [6]. Fractionation takes place within a trapezoidal channel without a stationary phase, hence FFF does not belong to the class of chromatographic separation techniques. The separation channel is filled with a carrier developing a parabolic flow profile. The velocity of the flow stream

varies as a function of distance from the channel walls (with the lowest velocity close to the channel walls). After the injection of a sample, it is focused to end up with a small sample band and as consequence the sample is accumulated to the bottom of the channel. Depending on the sample's diffusion coefficient sample fractions expand into different channel heights. Contrary to the sample diffusion a perpendicular field of adjustable strength is applied (in AF4 a perpendicular flow). Upon the establishment of equilibrium, the different sample fractions move in different channel heights and interact with different flow-profile velocities; thus separation/fractionation is achieved (see figure VII-2). Fractions containing constituents exhibiting a small diameter/molar weight elute prior larger ones (normal mode); though, if the diameter/molar weight exceeds a given value elution order is reversed (steric/hyperlayer mode). For further detailed theoretical consideration the reader is referred to the respective literature [e.g., 7].

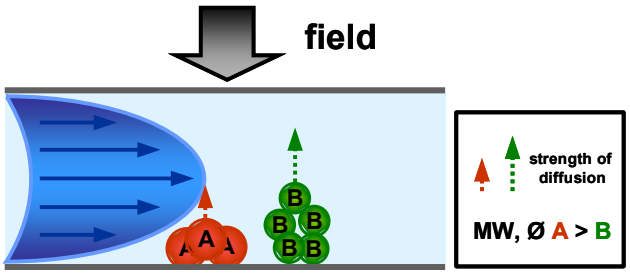

Figure VII-2: Simplified schematic separation principle in FFF - Interaction of parabolic flow-profile velocities, back-diffusion of particles and perpendicular field applied. (Scheme is not true to scale - fractionation takes place only in the lower 3-5% of the channel.)

Comparison HDC ⇔ FFF

To provide a general, comparative overview on the benefits and drawbacks of HDC and FFF several criteria are compiled and assessed within table VII-1:

Table VII-1: Direct comparison of pros & cons of HDC and FFF; Assessment is indicated via green – pros and red –cons color; sample dependent/under debate

criteria	HDC	FFF
instrument costs	low	high
effort method development	moderate	high (several parameters)
quantification - calibration	ionic fraction applicable	alternative strategy needed
sample interaction with system	quasi "stationary phase"	no stationary phase (but: possible membrane interaction)
detection of ionic fraction	enabled	disabled (lost via cross flow)
fractionation power	moderate	high
size resolution	smaller (up to 1.2 µm)	larger (up to 50 µm)
recovery	high (easy to determine)	moderate
on-line sample concentration	disabled	enabled
size calibration	irrespective of particle´s properties	in principle specific standards needed

On first sight, drawbacks of FFF prevail – though, at closer inspection several "weak" criteria were taken into account as well, e.g., asset costs, efforts needed for method development. Disregarding these kind of criteria pros and cons of both techniques are balanced. Mass-quantification and detection of ionic fractions is facilitated in HDC, while fractionation power and size range is elevated in FFF. Hence, the choice of the appropriate system depends on the application/information intended and both systems can be used in a complementary manner. For instance HDC can be used for determining the ratio between dissolved and particulate forms of the analyte and for obtaining a rough idea on the size distribution, while a more precise description of the size distribution can be obtained using AF4. However, with regard to the present study both systems are applicable.

VII.2 Participants and analytical measures

In total three attendees (#4, #5, #12) applied a fractionation system coupled on-line with a respective detector. One attendee made use of hydrodynamic chromatography (HDC) coupled to ICP-MS. Two attendees applied asymmetrical field-flow fractionation (AF4) either coupled on-line to UV/Vis and MALLS or ICP-MS. (Table VII-2).

VII.3 Sample preparation

Attendee #4 diluted the samples 1:100 by means of MilliQ water. Except sample 5 was diluted 1:10 upon filtration by means of a 1 µm PRFE filter to remove visible larger particles. Attendee #5 conducted sample sonication for 5 sec in a sonication bath @720W prior measurement. No dilutions were conducted. Attendee #12 conducted "vortex" mixing of the samples until resuspension of sedimented particles. Afterwards, samples were sonicated within a water sonication bath for 10 min and shaken prior sample injection. No sample dilution was carried out.

VII.4 Results and discussion

Table VII-2 lists the obtained results; in comparison table VII-3 lists the expected (theoretical) results upon mixing the samples.

Table VII-2: Obtained results of the three attendees: #4-HDC/ICP-MS; #5-AF4/UV/MALLS; #12-AF4/ICP-MS

Attendee	**#4**		**#5**		**#12**	
Sample	particle mL^{-1}	diameter [nm]	particle mL^{-1}	diameter [nm]	particle mL^{-1}	diameter [nm]
1	-	260	$9.7x10^{7}$	300	$1.8x10^{8}$	235
2	-	46	$4.0x10^{10}$	49	$3.0x10^{10}$	48
3	-	9	$9.6x10^{11}$	17	$3.8x10^{14}$	2
4	-	8/43/272	-	49/283	-	4/49
5	-	37/244	-	46/169/395	-	50/237
6 - blank	-	-	-	-	-	-

Table VII-3: Expected (theoretical) results upon sample mixing

	Expected values		
Sample	particle mL^{-1}	diameter [nm]	nano?
1	$3.6x10^{8}$	250	-
2	$4.5x10^{10}$	50	-
3	$5.7x10^{12}$	10	-
4	$1.7x10^{12}/2.3x10^{10}/7.2x10^{7}$	10/50/250	yes
5	$2.3x10^{9}/3.4x10^{8}$	50/250	yes
6 - blank	-	-	

Upon assessing the results it turns out that good agreement for the monodisperse samples among all three applied techniques exist. The conformity of HDC/ICP-MS results is the highest, while AF4/UV/MALLS slightly overestimate the largest and the smallest particles in size. Attendee #12 slightly underestimates the smallest particles in size, while sample 1 and 2 are nicely recovered. A possible reason for under- and overestimation of sizes in AF4 is most probably related to (i) an inappropriate channel-size calibration (refer also to table VII-1) due to missing appropriate size-calibration standards attendee #5 used polystyrene standards; attendee #12 applied AuNPs standards); (ii) charge repulsion effects between surface charge of the particles and the charge of the membrane. This is most probably the reason for the underestimation of sample 3 by attendee #12 – hence, upon charge repulsion particles elute earlier than expected.

As mention in table VII-1 in HDC any size-calibration standard can be applied for appropriate size-calibration; hence, possible effects related to surface properties of the particles used for calibration are negligible.
Having a closer look on results of samples 4 and 5 (bi- and trimodal mixture of AuNPs sizes) HDC identifies the right number of fractions and also appropriate size-determination was enabled. Only the smaller fraction in sample 5 (50 nm) was underestimated.

The results obtained by attendee #5 observed only two fractions on sample 4 and a further fraction in sample 5. Most probably (with regard to sample 4) the sensitivity of the UV/Vis or MALLS detector was not sufficient to detect the smallest fraction as well (indicated by a remark of the attendee). In terms of sample 5 a further larger fraction (395 nm) was detected – on basis of remarks from several attendees it is most likely that agglomerates/aggregates were formed within sample 5 that were detected as well. Attendee #12 detects only two fractions in sample 4, while the smallest fraction is underestimated in size (most probably to particle-membrane charge repulsion; mentioned above). Sample 5 is nicely matched by attendee #12.

Regarding the determination of the particle-number concentration only attendee #5 and #12 delivered values. Both attendees applied approximations for the calculation of particle-number concentrations: total mass of gold, the determined size and further factors were taken into account. Hence, only for the monodisperse samples a number-based concentration was calculated. Even though various approximations were applied a relatively good agreement among expected and determined values for sample 1 and 2 was achieved; given the fact that determined values for the diameter are included in these calculations the quality of the number-based results strongly depends on the quality of the determined diameter values. Hence, sample 3 is either under- or overestimated by attendee #5, respectively #12.

As a general result both HDC and AF4 deliver relatively good agreement regarding size-determination for AuNPs samples. Size deviations in AF4 are mostly related to inappropriate channel-size calibration (lack of sufficient standards) or particle-membrane repulsions leading to an earlier elution of size-fractions.

Given the fact that method development in AF4 is more laborious than in HDC we recommend a first quick screening of complex samples via HDC. First screening results can be embedded in method development of AF4. With regard to complex environmental matrix AF4 offers the benefit of (partial – smaller than cut-off of membrane) matrix removal – this is not the case for HDC analysis.

VII.5 EU Definition

For the transformation of mass-based to number-based concentrations approximations were applied – however, we recommend the application of a multi-detector approach to fulfill the demand from the EU definition of nanomaterials [8]; e.g., MALLS, UV/Vis, and ICP-MS detection. A promising approach becoming more and more popular is the combination of an appropriate fractionation system (e.g., HDC, AF4) and single particle ICP-MS (sp-ICP-MS). AF4/HDC offers fractionation while sp-ICP-MS delivers direct number-based quantification of particles within separated fractions.

References:

[1] A. J. McHugh and H. Brenner, Particle size measurement using chromatography. *Critical Reviews in Analytical Chemistry* 1984, **15**, 63-117.

[2] A. M. Striegel and A.K. Brewer, Hydrodynamic Chromatography. *Annual Review of Analytical Chemistry* 2012, **5**, 15-34.

[3] R.F. Stoisits, G.W. Poehlein and J.W. Vanderhoff, Mathematical modeling of hydrodynamic chromatography. *Journal of Colloid and Interface Science* 1976, **57**, 337-344.

[4] R. Tijssen, J. Bos and M.E. Van Kreveld, Hydrodynamic chromatography of macromolecules in open microcapillary tubes. *Analytical Chemistry* 1986, **58**, 3036-3044.

[5] M.S. Chun, O.O. Park and J.K. Kim, Flow and dynamic behavior of dilute polymer solutions in hydrodynamic chromatography. *Korean Journal of Chemical Engineering* 1990, **7**, 126-137.

[6] J.C. Giddings, *Sep. Sci.* 1966, **1**, 123-125.

[7] M. Schimpf, K. Caldwell, J.C. Giddings, Field-Flow Fractionation Handbook. *Wiley-Interscience, New York* 2000.

[8] European Commission, Commission recommendation of 18 October 2011 on the definition of nanomaterial (2011/696/EU). *Official Journal* 2011a, **L 275**, 38-40.

VIII Laser-induced breakdown-detection (LIBD)

VIII.1 Theoretical background of LIBD

Analysis of nanoparticles (NPs) by laser-induced breakdown-detection is based on the generation of dielectric breakdowns of suspended solid matter in the strong electric field of a focused pulsed laser beam and the subsequent detection of these breakdowns [1]. The method has not been commercially available until recently and thus is not in widespread use for environmental analysis. The method is highly sensitive. NPs in the low nm-range can be detected in concentrations down to the ng/L-range. Depending on the method of breakdown detection, discrete number-based particle size distributions or mean diameters can be obtained [1].

The method is not material specific, i.e. no information on the kind of material a NP consists of can be obtained. However, for different solid materials, a dependency of the signal on the type of material exists. While many types of materials exhibit similar breakdown behavior, certain materials can differ significantly in their breakdown behavior. As a LIBD system needs to be calibrated with reference particles of known sizes and concentrations, obtained results have to be considered as equivalent to the material used for calibration [1].

VIII.2 Participants and analytical measures

One attendee of the ICS applied LIBD (#7).

The LIBD system that was used by attendee #7 for analyzing the Au NP samples of the ICS is self-assembled based on the design developed by Walther et al. (2002) [2]. A pulsed Nd:YAG laser delivering a laser beam with a wavelength of 532 nm serves as light source. The laser pulses have an energy of up to 7 mJ. The pulse duration is 7 ns (full width at half maximum) and the pulse repetition rate is 20 Hz. Breakdowns are detected acoustically. Discrete particle size distributions are obtained by analyzing the number of occurring breakdown events depending on the laser pulse energy [3]. Calibration of the system has been carried out using polystyrene reference NPs in the size range from 20 to 1000 nm.

VIII.3 Sample preparation

Samples were diluted with ultrapure water and vortex mixed prior measuring. Different dilution factors were tested and used for each sample to meet the working ranges of the LIBD (Table VIII-1).

Table VIII-1: Dilution factors for LIBD measurements

	Minimum dilution factor	Maximum dilution factor
Sample 1	1:100	1:500
Sample 2	1:50	1:500
Sample 3	1:100	$1:10^5$
Sample 4	1:100	1:500
Sample 5	1:100	$1:10^5$

VIII.4 Results and discussion

The results for sample 1-5 are shown in Table VIII-2.

Table VIII-2: LIBD results of samples 1-5 and nominal Au NP sizes and concentrations

	$\text{Size}_{\text{measured}}$ [nm]	$\text{c(Au NP)}_{\text{measured}}$ [particles/mL]	$\text{Size}_{\text{nominal}}$ [nm]	$\text{c(Au NP)}_{\text{nominal}}$ [particles/mL]
Sample 1	**200**	**$2.0*10^8$**	250	$7.2*10^7$
Sample 2	**< 20**	**--**	50	$4.5*10^{10}$
Sample 3	**< 20**	**--**	10	$3.6*10^8$
Sample 4	**< 20**	**--**	10 50 250	$1.7*10^{12}$ $2.3*10^{10}$ $7.2*10^8$
Sample 5	**200**	**$2.6*10^8$**	50 250	$2.3*10^9$ $3.4*10^8$

In sample 1, 200 nm NPs with a concentration of $2.0*10^{11}$ particles/L have been measured. This is in the same range as the nominal size (250 nm) and concentration ($7.2*10^{10}$ particles/L) as expected based on the supplier's information. Differences might have been caused by the limited size resolution of the LIBD system in the size range > 100 nm and in differences in the breakdown behavior between Au NPs and polystyrene particles (which have been used for calibrating the system). Au NPs need a higher laser pulse energy for inducing breakdowns than polystyrene particles of same size.

In samples 2 and 3 no NPs with diameters larger than 20 nm could be detected. As Au NPs in the nm-range absorb light at wavelengths of approximately 530 nm (depending on the particle size), which is very close to the wavelength of the laser beam, the non-detection might have probably been caused by the attenuation of the laser

pulse energy in the Au NP containing sample. Due to this absorption in the focal volume of the laser beam the laser pulse energy was probably not sufficient for inducing breakdowns. Furthermore, interactions of the laser beam with citrate, which was present in the samples as stabilizing agent, could potentially lead to problems in detecting the Au NPs [4]. In sample 4, with a large fraction of 10 and 50 nm Au NPs, also no particles could be

detected. In sample 5, with a larger fraction of 250 nm particles, particles in the size range of 200 nm and a concentration of $2.6*10^{11}$ particles/L could be measured which is, similar to sample 1, in the same range as the nominal concentration and size of the largest particles (i.e. 250 nm in nominal size). In total, it is indicative that the presence of large fractions of Au NPs < 100 nm hinder reliable characterization of Au NP containing suspensions.

As only one participant of the ICS applied LIBD, no comparison of results obtained by different LIBD measurements was possible.

VIII.5 EU Definition

LIBD is highly sensitive to NPs and it delivers a number-based particle size distribution. Depending on the sample, no or only little sample preparation (removing of large-scale particles, dilution) is necessary. Thus, in principle, LIBD seems a promising tool for analyzing particle size distributions with respect to the decision if a material is "nano or not" based on the EU definition. However, as Au NP show plasmon resonance and absorb light in range of the (in this case) applied laser beam wavelength, detection and characterization of Au NP seem not to be reliable. Furthermore, more research is necessary to evaluate the influence of other water constituents and dispersing agents on the LIBD signal [4].

References:

[1] J.I. Kim, C. Walther, Laser-induced break down detection. In: Lead,J. and Wilkinson,K. (eds), Environmental colloids and particles: Behaviour, separation and characterisation. *John Wiley & Sons Ltd.* 2007, pp. 556-605.

[2] C. Walther, C. Bitea, W. Hauser, J.I. Kim, F.J. Scherbaum, Laser induced breakdown detection for the assessment of colloid mediated radionuclide migration. *Nuclear Instruments and Methods in Physics Research B* 2002 **195**, 374-388.

[3] C. Walther, S. Büchner, M. Filella, V. Chanudet, Probing particle size distributions in natural surface waters from 15 nm to 2 µm by a combination of LIBD and single-particle counting. *Journal of Colloid and Interphase Science* 2006, **301**, 532-537.

[4] N. Fedotova, R. Kaegi, J. Koch, D. Günther, Influence of dispersion agents on particle size and concentration determined by laser-induced breakdown detection. *Spectrochimica Acta Part B: Atomic Spectroscopy* 2015, **103-104**, 92-98.

IX Conclusions/recommendations/evaluation

In the following an assessment of the obtained results with regard to several aspects is undertaken. The aspects taken into account are related to the following questions deviated by the participants:

1- are the results from identical methods comparable? What are the reasons that lead to differences in the results?
2- are the results from different methods comparable? What are the possible reasons leading to differences in the results?
3- do you have recommendations in terms of data interpretation/assessment for specific methods (e.g., mass-based concentration vs. number-based concentration; means vs. mode model;…)?
4- which are the benefits of each method (e.g., suitability for mono-/polydisperse samples; concentration range;…)?
5- is the respective method suitable for a decision nano: YES/NO in terms of the EU definition?
6- in general: is the EU definition suitable (especially with regard to "simple" AuNPs samples)?
=> are further guidelines with regard to the applied methods needed (e.g., sample preparation,…)?
7- is a technique/minimal set of techniques available which is self-sufficient to decide whether a sample is a nanomaterial or not according to the EU definition?

1- Are the results from identical methods comparable? What are the possible reasons leading to differences in the results?

The **NTA** analyses results are in good agreement among each other, at least for the single-size standards 50 nm and 250 nm; except for the 10 nm standards. Within sample 4 (mixture) most attendees detected 50 nm, although 10 nm is the main fraction within the suspension – most probably due to limits of detection. As several attendees observed sedimentation/agglomeration/aggregation processes 250 nm fraction was not observed within sample 4. Within sample 5 the main size fraction was 250 nm which was detected by most of the attendees. In general the data were comparable for NTA or at least in the same order of magnitude. Within **NTA** approaches mainly technical reasons were identified leading to different results: (i) camera is not sensitive enough for small particles, (ii) the chosen set of gain and shutter is not adequate, (iii) different systems were applied by the users.

For the **sp-ICP-MS** results, the 250 nm fraction was not always detected within sample 1 – this was the case for attendees using a sector-field ICP-MS (most probably due to higher sensitivity and detector signal saturation). On the other hand within sample 3 the 10 nm fraction was detected by means of users applying a sector field instrument; though for attendees applying a quadrupole-based ICP-MS distinction from background signals was hardly to achieve, hence 10 nm fraction was in most cases not detectable, respectively size was overestimated. 50 nm fraction was reproducibly determined by all attendees. Differences in the results stem mainly from instrumental factors such as: sensitivity, affecting lower and upper size-limits of nanoparticles (sector field ICP-MS vs. quadrupole ICP-MS); nebulization efficiency determination: to deduce the number-concentration from the number of peaks from raw-data. A further source of uncertainty is the difference between nominal and effective dwell times.

DLS produce highly reproducible and reliable measurements for monodisperse nanoparticle suspensions (usually with diameters higher than 20 nm), hence, the results observed by the attendees are in good agreement among each other. However, using DLS for the analysis of mixtures of monodisperse nanoparticles is difficult due to high dependency on the mixing ratio of the particles in suspensions; smaller particles are "masked" in the presence of larger particles, hence, size is biased. Measurement parameters (e.g. refractive index) are a crucial parameter during analysis.

The **AFM/NTA** results are in good agreement for the 10 nm and 50 nm particles. Largest absolute deviations were observed among the analyses of the 250 nm particles within monomodal suspensions. Within sample 4 most attendees detected the 10 and 50 nm fraction; however, the 250 nm fraction was only observed by one attendee. Results for sample 5 were in relatively good agreement. One attendee deployed AFM; sizes for samples 4, 5 were underestimated. Differences in results are causes by the deviation of the particles' shapes from ideal spheres and thus reported diameter values might be operator biased in the case of manual image analysis. Since sample preparation affects the results, differences in the way of preparing the samples are most likely the major reason for the differences of the reported results.

The determination of the total gold concentration was conducted by means of **ICP-MS/ICP-OES** analysis. The results obtained by the attendees were in most cases in good agreement. Mostly aqua regia digestion of the Au NPs was conducted. The main reason for the deviation of the observed results within **ICP-OES/-MS** analyses is related to differences in sample preparation (i.e. the digestion method) - total decomposition of the Au NPs is needed and stabilization of the gold in solution by chloride ions is mandatory.

The comparison of **HDC/FFF** results with regard to the size determination of monomodal samples (sample 1-3) was in good agreement among the attendees. HDC/ICP-MS matched all polymodal samples (sample 4 + 5) in a good way. One attendee deployed FFF/UV-VIS; the 10 nm fraction in sample 4 was not identified (most probably due to lack of sensitivity) and a 3rd larger fraction within sample 5 was detected (maybe due to agglomeration/aggregation). One attendee applied FFF/ICP-MS and underestimated the size of the 10 nm fraction in sample 4 (most probably due to slight error in size-channel calibration). Furthermore, a larger size fraction in sample 4 was not detected; fraction-size determination in sample 5 was in good agreement with HDC/ICP-MS results. Number-based concentration determination were in good agreement among each other for samples 1 & 2; while for sample 3 a deviation from the expected value occurred (most probably due to channel calibration). Deviation of results in **HDC/FFF** is related due to several reasons: If the size determination within FFF is conducted upon channel calibration, specific standards are needed - otherwise over-/underestimation of the results occur. HDC does not need specific standards; hence, e.g., certified polysterene standards can be used. Application of a appropriate light scattering detector (MALS, DLS) can reduce the uncertainties related to potential different behavior between the analyte and the standard used. The determination of the number-size concentration in FFF is based on several estimations made (e.g., spherical shape of NPs); upon this a quantitative information of the total gold content in each fraction is linked with the experimentally determined diameter of the Au NPs. On basis of these information the number concentration AuNPs in each fraction is deduced.

2- Are the results from different methods comparable? What are the possible reasons leading to differences in the results?

A comparison of the results obtained by the different methods is shown in Figure IX-1 and Figure IX-2. Displayed results are averages of the different reported values for a specific method.

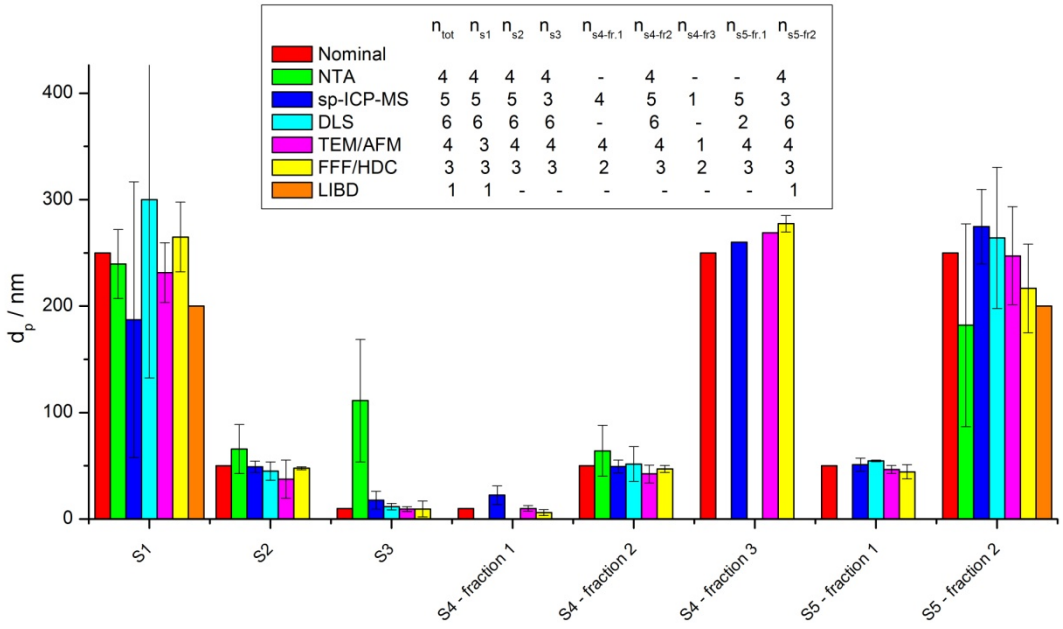

Figure IX-1: Comparison of obtained diameters for the different samples. Displayed results are the averages of the reported diameters obtained by the respective methods. Numbers in the legend indicate how often the fractions were detected by the respective method.

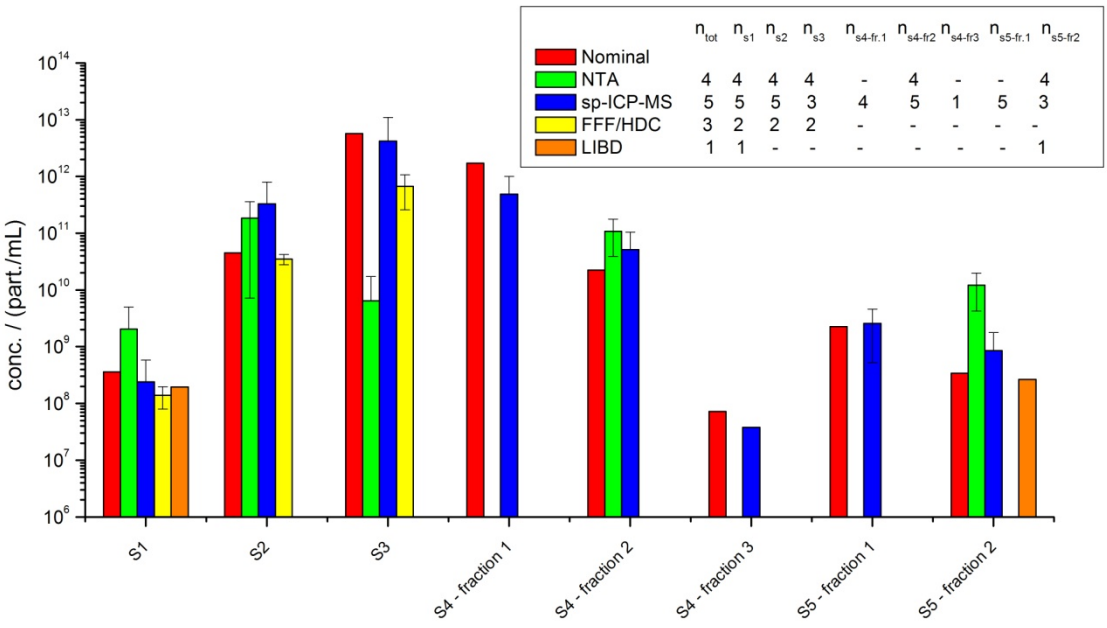

Figure IX-2: Comparison of obtained concentrations for the different samples. Displayed results are the averages of the reported concentrations obtained by the respective methods. Numbers in the legend indicate how often the fractions were detected by the respective method.

Despite the different physical principles of the applied methods, the reported diameters agree fairly well between the different methods, and are comparable with the nominal sizes of the Au NPs. For sample 3, the results of NTA deviated from the other obtained results, which is due to one measured diameter of 630 nm by one attendee (not excluded from averaging the results). Deviations of the results in between the methods are not only due to

different physical principles, but also due to uncertainties when converting obtained measurement signals to diameters. However, obvious differences exist in the capabilities of the different methods to detect several particle populations in polydisperse samples. While DLS and NTA were mostly only capable of detecting one particle size in the polydisperse samples 4 and 5, application of sp-ICP-MS or FFF/HDC enabled the detection of several particle populations (even though, in general, not all particle populations could be detected within one sp-ICP-MS measurement due to instrumental limitations; refer to section II).

The deviations in reported particle concentrations are much larger between the different methods than for the diameters. Results differ by up to some orders of magnitude, and also less methods are capable of determining number-based particle concentrations. In addition to the different physical principles, differences in sample preparation (e.g. dilution, shaking), sedimentation of particles, and conversion to number-based results have contributed to differences in the results.

3- Do you have recommendations in terms of data interpretation/assessment for specific methods (e.g., mass-based concentration vs. number-based concentration; means vs. mode model;…)

Within **NTA** it seems crucial not only to look to the mean and mode values, but also critically observe the distribution curve in order to evaluate the presence or not of small populations of particles with different sizes.

Within **sp-ICP-MS** it is mandatory to collect large number of data points (about 10,000) to end up with good statistical values.

In case of **AFM/TEM** algorithms to convert data become redundant; given the fact that images are directly number-based.

A good measurement of NPs' constitutive element(s) concentration(s) by ICP-OES/-MS requires a 100% NPs dissolution. The best protocol for AuNPs dissolution would be first ultrapure HCl + sonication + HNO_3 (to get aqua regia) then either microwave or hot plate digestion. Evaporation then dilution in HCl 1% before analysis.

4- Which are the benefits of each method (e.g., suitability for mono-/polydisperse samples; concentration range;…)

In case of **NTA** the method is less prone to impurities/matrix (compared to, e.g., DLS). Furthermore, the particles are (indirectly) visible: hence, a possible heterogeneity is observable. Thus, an ideal concentration is adjustable. In comparison to, e.g., DLS higher LODs are obtained.

Sp-ICP-MS appears as the only method that could provide reasonable estimates of particle number concentration - even in polydisperse samples (which is beneficial over, e.g., DLS; NTA) - as long as the particles are detectable (with regard to limits of detection). But, for the sake of completeness it must also be stated that the nominal concentrations are not necessarily the most accurate ones as nanoparticles tend to stick to glass walls over time, thus decreasing in number concentrations.

In case of **DLS** the method is simple. However, critical aspects mentioned previously need to be taken into account.

Even in case of polydisperse and polymodal samples analysis by means of **AFM/TEM** is possible as larger particles do not negatively interfere smaller ones (compared to, e.g., DLS, NTA).

The benefit of **ICP-OES/-MS** is the fast as well as reliable determination of total Au concentration; hence, in combination with data from complementary sizing techniques further hints for number-based concentrations are obtainable. Furthermore, the results obtained allow for a controlling of stock suspensions at least for elemental concentration (keeping possibly dissolved ionic fractions in mind).

HDC or **FFF** have the great advantage of having no problem to resolve the different size fractions as soon as the sizes remain fairly different. The complexity of polydisperse samples is thus reduced allowing a greater flexibility and robustness compared to non-separating techniques.

5- Is the respective method suitable for a decision nano: YES/NO in terms of EU definition?

NTA as well as **DLS** are not suitable for the decision, if a sample is a nanomaterial or not, due to interference of larger particle fractions on the light scattering signals of smaller particle fractions.

Sp-ICP-MS offers the possibility to determine both size and number concentration with high accuracy. Hence, sp-ICP-MS is applicable to the EU-nano definition, if NPs present in a sample consist of elements measurable by ICP-MS (as shown for the Au NPs in this ICS). However, some limitations need to be taken into account, when NPs are below or above a given size limit (due to lack of sensitivity or linearity). But, technical developments are ongoing most probably tackling these limitations.

The suitability of **AFM/TEM** with regard to the decision whether a sample is a nanomaterial or not depends on the sample preparation strategy; if the approach is representative then AFM/TEM is suitable.

HDC/FFF are principally suitable for the EU nano-definition depending on experimental setup/detector applied. One major challenge in FFF are lacking size-standards. In HDC size calibration is easier to conduct.

6- in general: is the EU definition suitable (especially with regard to "simple" AuNPs samples)?

Both, sample 4 and 5 were nominally a "nanomaterial" based on the EU definition. Table IX-1 shows the decisions by the attendees, if samples 4 and 5 are "nanomaterials". Not all methods delivered results that enabled a decision if the samples are "nano or not". When applying DLS, ICP-MS/OES and LIBD (in the case of Au NPs), none of the attendees could decide whether samples 4 or 5 were "nano or not".

Table IX-1: Decisions by attendees if polydisperse samples (sample 4+5) are nanomaterials or not based on the EU definition

	NTA		**Sp-ICP-MS**		**AFM/TEM**		**AF4/HDC**	
Nano?	yes	no	yes	no	yes	no	yes	no
Sample 4	4	0	5	0	3	0	2	0
Sample 5	2	2	5	0	2	1	2	0

Sample 4 was always correctly identified as a nanomaterial, when a decision was stated. In the case of sample 5, it was reported both, that the sample is a nanomaterial and that it is not a nanomaterial. However, the majority identified the sample correctly as a nanomaterial. In the case of Au NPs, it appears that by using a combination of TEM/AFM and (AF4/HDC)-sp-ICP-MS a sample can be reliably identified as a nanomaterial or not. Thus, the EU definition is applicable and suitable in this case.

However, this ICS shows that only certain analysis methods are applicable for the EU definition, even for "simple systems". The varying results of this ICS performed on samples as simple as Au NPs highlight that the use and/or the application of this definition for answering to the question "is that material a nanomaterial?" remains arduous and challenging given the existing analytical tools. This especially applies if samples increase in complexity and become more heterogenous. In this case, the analytical requirements would potentially not be fulfilled by the existing technique.

7- is a technique/minimal set of techniques available which is self-sufficient to decide whether a sample is a nanomaterial or not?

This ICT reveals that, in general, none existing technique is able, if used alone, to answer to this question. Even in the case of "simple systems", such as reference Au NPs suspended in deionized water, several techniques need to be combined to obtain reliable results.

Based on the outcome of this ICS, following analysis chain is suggested as an possible approach to determine whether a sample is "nano or not":

1- Measure particle size by DLS and total element concentration in undiluted sample,

2- Decide on necessary dilutions if any,

3- Perform a total particle deposition on a TEM grid (e.g., with centrifugation according to the elements density assuming a "worst case" size),

4- Do automated TEM analysis,

5- For orthogonal confirmation, do sp-ICP-MS (if the element to be analyzed is suitable of sp-ICP-MS),

6- Use time intensive separation techniques such as HDC or FFF only when really necessary,

7- In addition, for each quantitative technique, assess method reproducibility for each sample.

However, for samples that are highly complex, heterogeneous and contain NPs of various composition (such as environmental samples), even the proposed analytical chain might not be sufficient for obtaining reliable results. It has to be emphasized that the above suggested analytical chain is highly demanding in terms of time, cost and analytical equipment. Thus investigations into whether a sample is a nanomaterial or not based on the current suggestion of the EU definition can currently hardly be performed on a routine basis.

Acknowledgements

The attendees of the ICS would like to thank Norman for funding the Au NP standards and COST for funding the workshops and meetings for planning the ICS and discussing its results.